

**IS675**

**Deep Learning for Business**

**DEEP LEARNING FOR MUSCULOSKELETAL  
RADIOGRAPH ANALYSIS**

**&**

**MACHINE LEARNING ANALYSIS FOR FORMULA 1**

**Team 7**

**By**

**Shoaeb Nawab Shaik  
Rithika Goud Pabathi  
Yesha Ajaybhai Doshi  
Visnupriyan Kumarraja**

**Professor  
Mostafa Amini**



CALIFORNIA STATE UNIVERSITY

**LONG BEACH**

College of Business

## Table of Contents

<b>Unstructured Data .....</b>	<b>4</b>
<b>Introduction to Project .....</b>	<b>4</b>
Background .....	4
Problem Statement .....	4
Impact on Business .....	5
<b>Dataset Description: MURA .....</b>	<b>6</b>
Dataset Composition .....	6
Use Case .....	6
Importance .....	6
<b>Dataset Dictionary .....</b>	<b>7</b>
Data Distribution .....	7
<b>Feature Engineering .....</b>	<b>9</b>
Data Transformation .....	9
Scaling .....	10
Feature Selection .....	10
<b>Model Building .....</b>	<b>10</b>
Data Splitting .....	10
Evaluation of Model .....	11
<b>Modeling .....</b>	<b>12</b>
Densenet169 Model: .....	12
RESNET Model: .....	13
<b>Deep Learning Techniques .....</b>	<b>14</b>
DenseNet169 Results and Discussion .....	14
<b>Forearm .....</b>	<b>14</b>
Iteration 1 .....	14
Iteration 2 .....	15
Iteration 3 .....	17
Iteration 4 .....	18
<b>Shoulder .....</b>	<b>20</b>
Iteration 1 .....	20
Iteration 2 .....	21
Inference .....	23
<b>RESNET Results and Discussion .....</b>	<b>24</b>
<b>Machine Learning Techniques .....</b>	<b>26</b>
Random Forest classifier .....	26
Shoulder .....	26
Forearm .....	28
Logistic Regression Model .....	30
Support Vector Machine (SVM) .....	32
<b>Business and Clinical Impact .....</b>	<b>34</b>
<b>References .....</b>	<b>35</b>
Datasets .....	35
Research Papers .....	36

<b>Structured Data .....</b>	<b>37</b>
<b>Abstract.....</b>	<b>37</b>
<b>Background .....</b>	<b>38</b>
<b>Problem Statement .....</b>	<b>40</b>
<b>Impact on Business.....</b>	<b>40</b>
<b>Data set and Domain.....</b>	<b>42</b>
<b>Data Selection Criteria .....</b>	<b>43</b>
<b>Exploration data analysis .....</b>	<b>44</b>
Lewis Hamilton's Performance Over Time: .....	44
Mercedes' Constructor Standings Over Time .....	45
Race Finish Position Distribution by Top 5 Constructors (All Years) .....	46
Driver Finishing Positions at Monaco Circuit .....	47
Top 10 Drivers by Wins .....	48
Top 10 Drivers by Points .....	49
Average Qualifying Position for Top Drivers .....	50
Pit Stop Times Distribution .....	51
Number of Constructors vs Average Pit Stop Time .....	52
Number of Race Tracks vs Average Pit Stop Time .....	53
Pit Stop Durations Over Time by Constructor .....	54
Pit Stop Durations Over Time by Constructor (Second Image) .....	55
Average Race Pit Stop Durations by Race Circuit .....	56
Average Race Pit Stop Durations by Circuit (Simplified) .....	57
Pit Stop Durations by Race Circuit (Boxplot) .....	58
Pit Stop Durations by Constructor for 2021 Season .....	59
Pit Stop Durations by Constructor from 2011 to Date .....	60
Average Pit Stop Durations by Constructor .....	61
Total Time Spent in Pit Lane by Circuit .....	62
Total Time Spent in Pit Lane by Circuit .....	63
Total Time Spent in Pit Lane by Circuit (Revised) .....	64
Average Race Percentage in the Pit Lane by Race Circuit .....	64
Pit Stop Duration Distribution .....	65
Average Pit Stop Time by Constructor .....	66
Average Pit Stop Time vs. Number of Wins .....	67
<b>Models Implemented .....</b>	<b>68</b>
RandomForestClassifier:.....	68
Support Vector Regressor (SVR):.....	68
Ridge Regression:.....	69
DecisionTreeRegressor:.....	70
Simulation of Race Strategies:.....	70
Key Outcomes:.....	71
<b>Conclusion .....</b>	<b>71</b>
<b>References .....</b>	<b>72</b>

# Unstructured Data

## Introduction to Project

### Background

Musculoskeletal conditions are a significant global health challenge, affecting over 1.7 billion people annually and leading to severe pain and disability. These conditions account for millions of emergency department visits and represent the most common cause of chronic pain worldwide. Diagnosing musculoskeletal abnormalities often involves interpreting radiographic studies, which requires specialized expertise and can be time intensive. However, radiologists frequently experience high workloads, which may lead to fatigue and decreased diagnostic accuracy over time.

Advancements in machine learning and deep learning have shown promising potential in aiding medical diagnosis. By leveraging datasets such as MURA, a large dataset of musculoskeletal radiographs labeled by radiologists, models can be trained to detect abnormalities with efficiency and accuracy comparable to human experts. These models not only improve diagnostic speed but also support radiologists by highlighting abnormalities, reducing errors, and ensuring standardized quality across healthcare systems.

### Problem Statement

The diagnosis of musculoskeletal conditions through radiographic imaging faces several critical challenges that hinder effective patient care and diagnostic efficiency:

**Prolonged Diagnosis Processes:** Patients often endure lengthy diagnostic cycles involving multiple imaging procedures, delaying the confirmation of conditions such as fractures or degenerative changes.

**Radiologist Fatigue and Overload:** The increasing volume of radiographic studies, combined with a global shortage of radiologists, results in excessive workloads. This can lead to diagnostic delays and a decline in accuracy due to fatigue.

**Inconsistent Diagnostic Accuracy:** Variability in expertise and fatigue-induced errors among radiologists can result in inconsistent interpretations, potentially affecting timely and accurate patient care.

**Limited Accessibility:** In underserved or remote areas, access to skilled radiologists is often unavailable, delaying diagnoses and impacting patient outcomes.

**Rising Healthcare Costs:** Inefficiencies in the diagnostic process, including the need for repeat imaging or second opinions, contribute to escalating healthcare expenditures.

This project addresses these challenges by leveraging deep learning techniques to automate the abnormality detection process in musculoskeletal radiographs. By utilizing the MURA dataset, a large and publicly available dataset of radiographs labeled by expert radiologists, the proposed solution aims to deliver a robust diagnostic tool. This tool will not only enhance the accuracy and speed of abnormality detection but also support radiologists by reducing their workload and improving diagnostic consistency, ultimately advancing patient care outcomes.

## **Impact on Business**

From a business perspective, this project addresses critical needs in the healthcare domain:

**Efficiency in Diagnostics:** Automating abnormality detection reduces the time radiologists spend on normal studies, allowing them to focus on complex cases. This leads to faster patient management and increased throughput in diagnostic centers.

**Cost Reduction:** By improving diagnostic accuracy and efficiency, healthcare providers can reduce costs associated with repeat imaging and delayed treatments.

**Scalability:** The proposed solution can be deployed in high-volume imaging centers and remote areas, expanding access to quality diagnostics and enabling equitable healthcare services.

**Enhanced Decision-Making:** With visual insights like Class Activation Maps (CAMs) highlighting abnormalities, clinicians gain additional tools to make informed decisions, ultimately improving patient outcomes.

**Market Potential:** The integration of AI in medical imaging is a rapidly growing field. By demonstrating its value, this project can attract investments and collaborations, positioning healthcare providers at the forefront of innovation.

## **Dataset Description: MURA**

MURA (Musculoskeletal Radiographs) is a large and publicly available dataset designed for detecting abnormalities in musculoskeletal radiographs of the upper extremities. The dataset comprises 40,561 images from 14,863 studies, representing one of the largest collections of radiographs for abnormality detection. Each study is labeled as either normal or abnormal based on expert radiologist assessment.

### **Dataset Composition**

MURA includes radiographs of seven anatomical regions of the upper extremities:

Elbow

Finger

Forearm

Hand

Humerus

Shoulder

Wrist

The dataset contains a total of 14,863 studies, distributed as follows:

9,045 studies are normal

5,818 studies are abnormal

This distribution provides a balanced representation of the diagnostic challenge, ensuring sufficient data for both training and testing machine learning models.

### **Use Case**

The primary task associated with MURA is binary classification, where the objective is to classify radiographic studies as "normal" or "abnormal." The dataset is well-suited for developing and benchmarking machine learning and deep learning algorithms for medical imaging.

### **Importance**

MURA provides an excellent platform for advancing AI-based diagnostic tools. It supports the development of algorithms that can:

- Assist radiologists in detecting musculoskeletal abnormalities efficiently.

- Improve diagnostic accessibility in areas with limited radiology expertise.
- Enhance diagnostic speed and accuracy in clinical settings.

This dataset serves as a critical resource for both researchers and practitioners in the medical imaging domain.

## Dataset Dictionary

The MURA dataset includes radiographic studies of the upper extremities, each labeled as either normal or abnormal by board-certified radiologists. The dataset is organized into seven anatomical regions, with corresponding attributes to facilitate data analysis and modeling. Below is a detailed description of the dataset structure and attributes:

Attribute	Description
Study ID	A unique identifier for each radiographic study.
Patient ID	A unique identifier for the patient associated with the study (de-identified for privacy).
Region	The anatomical region imaged in the study (e.g., Elbow, Wrist, Shoulder).
View	The angle or perspective of the radiograph (e.g., frontal, lateral).
Label	Binary classification indicating whether the study is <b>normal (0)</b> or <b>abnormal (1)</b> .
Image Count	The number of radiographic images (views) included in the study.
Dataset Split	Indicates whether the study belongs to the training, validation, or test set.

## Data Distribution

The dataset is split into three subsets for modeling and evaluation:

Training Set: Includes the majority of studies for model training.

Validation Set: Used for hyperparameter tuning and intermediate evaluations.

Test Set: Reserved for final model performance evaluation against benchmark radiologist interpretations.

Example Data Record

Below is an example of how the data may be structured:

Study ID	Patient ID	Region	View	Label	Image Count	Dataset Split
S001	P12345	Wrist	Frontal	1 (Abnormal)	2	Training
S002	P12346	Elbow	Lateral	0 (Normal)	1	Validation

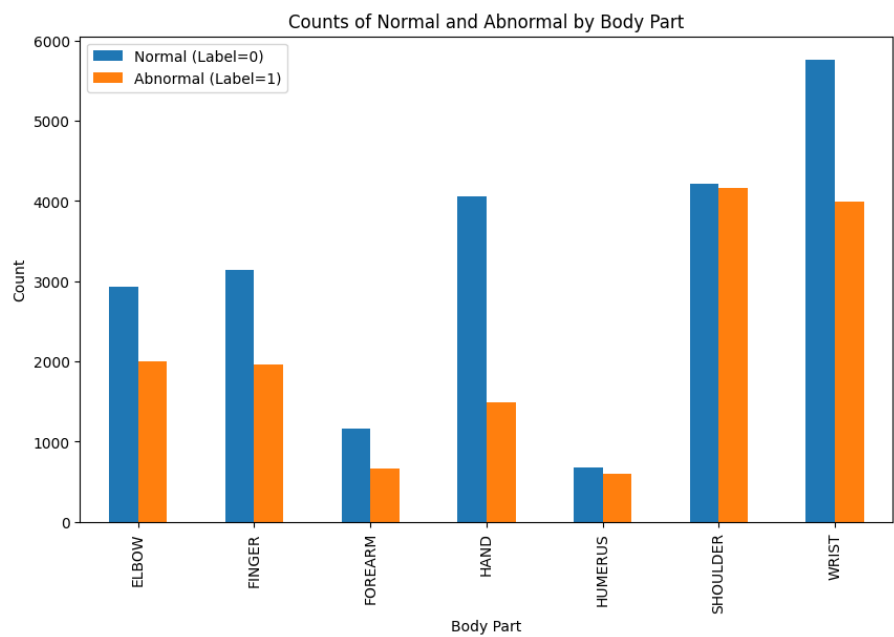


Figure 1 Body parts in the Dataset



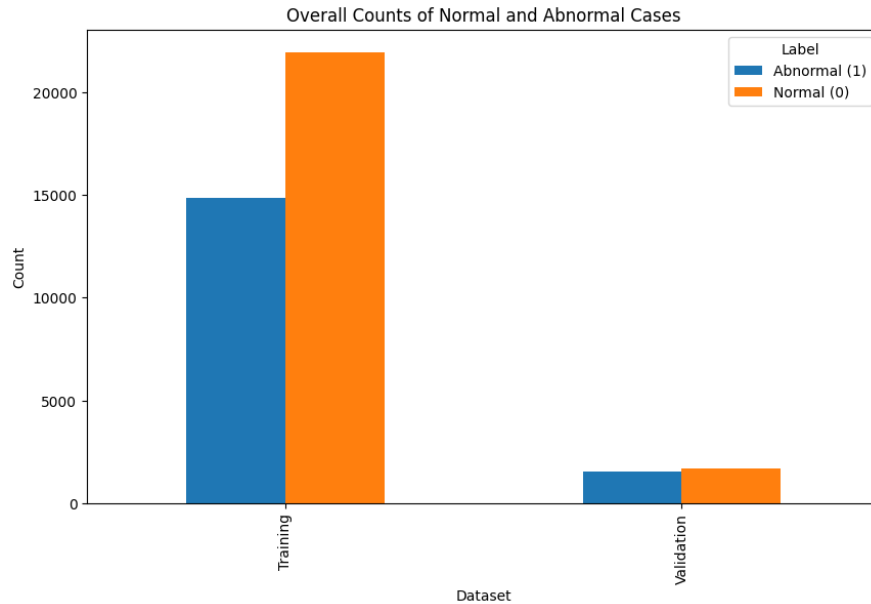


Figure 2 Labeled Items

## Feature Engineering

### Data Transformation

For the MURA dataset, data transformation is a crucial step to ensure the model performs effectively and generalizes well. The radiographs in this dataset were labeled manually as "Normal" or "Abnormal," providing the necessary ground truth for classification tasks. To standardize the data and prepare it for the DenseNet-169 deep learning model, several transformations were applied:

**Resizing:** All radiographs were resized to 320x320 pixels to ensure consistent input dimensions.

**Data Augmentation:** Augmentations such as random horizontal flipping and random rotations (up to 30 degrees) were applied to simulate real-world variations in imaging conditions. This enhances the model's ability to generalize across unseen data.

**Grayscale Conversion:** All images were converted to grayscale to simplify processing while retaining critical diagnostic information.

**Normalization:** Images were normalized using the ImageNet mean and standard deviation values. This aligns the data distribution with the pretrained DenseNet-169 model's expectations.

These transformations ensure that the data is in a format suitable for training and testing the model, improving robustness and performance.

## **Scaling**

Uniform scaling of pixel intensity values is essential for stable training and effective gradient-based optimization. The grayscale images were normalized to have a consistent mean and standard deviation using the `transforms.Normalize` function. The normalization parameters were derived from the ImageNet dataset (mean: 0.485, std: 0.229) to ensure compatibility with DenseNet-169's pretrained weights. This process not only accelerates the model's convergence but also stabilizes the training dynamics by standardizing the input data distribution.

## **Feature Selection**

Feature selection is inherently handled by the convolutional layers of the DenseNet-169 model. These layers identify and prioritize key regions within the radiographs that contribute to abnormality detection. The network utilizes its architecture to focus on diagnostically significant features, such as fractures, degenerative changes, and other abnormalities, while minimizing irrelevant information. Additionally, by limiting the number of image views per study to a maximum of three, the model avoids redundant computations and emphasizes the most informative perspectives. This strategy enhances the model's efficiency and its ability to generalize across varying cases.

## **Model Building**

### **Data Splitting**

The MURA dataset is divided into training and validation subsets to facilitate model development and unbiased evaluation. The training set constitutes most of the data and is used to train the model, while the validation set is employed for hyperparameter tuning and performance monitoring. Specifically:

Training Set: Contains the majority of the labeled studies for model learning.

Validation Set: Represents a smaller portion of the dataset, ensuring reliable evaluation during training.

This split ensures that the model learns to generalize across varying cases while retaining a representative evaluation subset. Consistent splitting is achieved through predefined CSV files, ensuring reproducibility.

## Evaluation of Model

### Evaluation Metrics

The evaluation of the DenseNet-169 model for medical image classification involves the use of the following metrics to measure performance:

#### Confusion Matrix:

The confusion matrix provides a detailed breakdown of the model's performance by showing:

**True Positives (TP):** Cases correctly classified as "Abnormal."

**True Negatives (TN):** Cases correctly classified as "Normal."

**False Positives (FP):** Cases incorrectly classified as "Abnormal."

**False Negatives (FN):** Cases incorrectly classified as "Normal."

This matrix highlights the model's strengths and weaknesses in distinguishing between the two classes.

#### Accuracy:

Accuracy measures the proportion of correctly classified cases across all samples. It is calculated as:

$$Accuracy = \frac{True\ Positives + True\ Negatives}{Total\ Samples}$$

Accuracy provides a general performance overview but can be misleading if the dataset is imbalanced.

#### Classification Report:

This report includes precision, recall, and F1 scores for both "Normal" and "Abnormal" classes, offering deeper insights into model performance for each category.

#### Precision:

Precision measures the proportion of correct positive predictions out of all predicted positives. It is calculated as:

$$Precision = \frac{True\ Positives}{True\ Positives + False\ Positives}$$

High precision indicates that the model has a low false positive rate.

### **Recall:**

Recall, also known as sensitivity, measures the proportion of actual positives correctly identified by the model. It is calculated as:

$$Recall = \frac{True\ Positives}{True\ Positives + False\ Negatives}$$

High recall indicates that the model misses very few actual positives.

### **F1 Score:**

The F1 score is the harmonic mean of precision and recall, providing a balanced measure of both metrics, especially useful when dealing with imbalanced datasets. It is calculated as:

$$F1\ Score = 2 \times \frac{Recall \times Precision}{Precision + Recall}$$

A higher F1 score indicates that the model performs well in identifying both classes effectively.

These metrics provide a comprehensive evaluation of the DenseNet-169 model's performance, enabling detailed analysis and comparison with other models. For this project, these metrics were computed and analyzed to understand the model's strengths and areas for improvement in classifying radiographs as "Normal" or "Abnormal."

## **Modeling**

### **Densenet169 Model:**

A DenseNet-169 convolutional neural network (CNN) is utilized for modeling due to its proven ability to extract spatial hierarchies and significant features from image data. The DenseNet-169 architecture is modified to accept grayscale images and output binary predictions (normal or abnormal). Key modifications include:

Replacing the initial convolutional layer to accommodate single-channel grayscale inputs.

Adapting the classifier layer to a binary output with a sigmoid activation function for probability estimation.

The DenseNet-169 model, known for its strong feature extraction capabilities, is used in this project with ImageNet pretrained weights to enhance performance on limited data. The model's first convolutional layer is modified to accept grayscale images, and the classifier is tailored for binary output using a sigmoid activation to predict normal or abnormal radiographs. Training is optimized with the Adam optimizer and Binary Cross-Entropy Loss to minimize classification errors, while data augmentation techniques like rotation and flipping improve generalization. The model processes up to three views per study, combining predictions to output a single abnormality probability, ensuring comprehensive analysis of each case. Performance is evaluated using metrics such as loss, precision, recall, F1 score, and a confusion matrix for detailed insights.

### **RESNET Model:**

A ResNet-50 convolutional neural network (CNN) is employed for modeling due to its robustness in handling complex image data and its proven efficiency in extracting hierarchical features. The ResNet-50 architecture is modified to accept grayscale inputs and output binary predictions (normal or abnormal).

Adjusting the first convolutional layer to accommodate single-channel grayscale images.

Modifying the final fully connected layer to produce a binary output with a sigmoid activation function for probability estimation.

Using pretrained ImageNet weights, the ResNet-50 model leverages transfer learning to adapt effectively to the MURA dataset. Training is performed using the Adam optimizer and Binary Cross-Entropy Loss to minimize classification errors, with data augmentation techniques like flipping and rotation applied to improve model generalization. The model outputs a single abnormality probability per study, ensuring accurate classification, and performance is assessed using metrics such as precision, recall, F1 score, and a confusion matrix.

# Deep Learning Techniques

## DenseNet169 Results and Discussion

### Forearm

#### Iteration 1

#### Training Performance

The DenseNet-169 model was trained for 5 epochs with the following hyperparameters:

- **Learning Rate:** 0.0001
- **Optimizer:** Adam
- **Loss Function:** Binary Cross-Entropy Loss
- **Batch Size:** 32

The training loss decreased to 0.3331 by the fourth epoch before slightly increasing to 0.3777 in the fifth, indicating convergence with minor fluctuations.

#### Evaluation Metrics

- **Accuracy:** 75%
- **Normal Class:** Precision = 68%, Recall = 97%, F1 = 80%
- **Abnormal Class:** Precision = 94%, Recall = 52%, F1 = 67%

#### Insights

- The model performed well in identifying "Normal" cases (high recall, 97%) but struggled with "Abnormal" cases (low recall, 52%).
- Data augmentation techniques like flipping and rotation improved generalization, but class imbalance impacted performance.

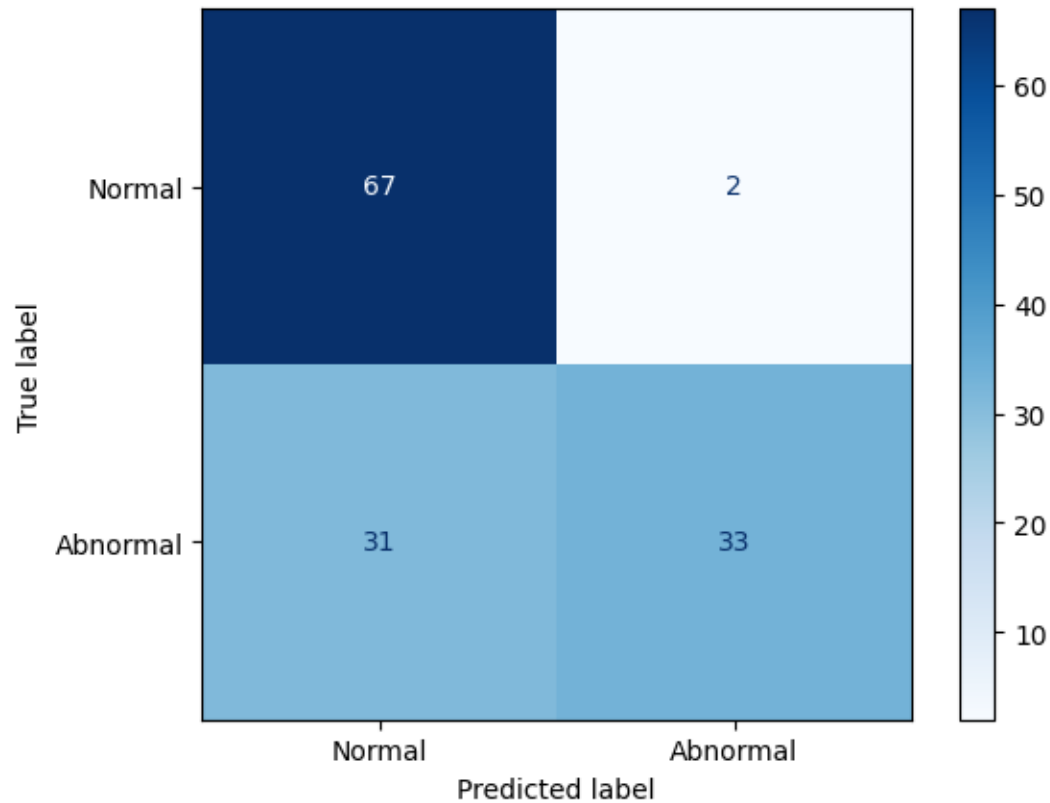


Figure 3 Iteration 1

## Iteration 2

### Training Performance

The DenseNet-169 model was trained for 15 epochs with the following hyperparameters:

- **Learning Rate:** 0.00001
- **Optimizer:** Adam
- **Loss Function:** Binary Cross-Entropy Loss
- **Batch Size:** 32

The training loss consistently decreased over the epochs, starting at 0.3420 in the first epoch and reaching 0.2548 by the 15th epoch, indicating steady convergence and improved model performance.

### Evaluation Metrics

- **Accuracy:** 77%

- **Normal Class:** Precision = 72%, Recall = 91%, F1 = 81%
- **Abnormal Class:** Precision = 87%, Recall = 62%, F1 = 73%

### Insights

- The model exhibited strong performance in detecting "Normal" cases, achieving a high recall (91%), meaning most normal radiographs were correctly identified.
- While the precision for the "Abnormal" class was high (87%), the recall (62%) indicates the model missed some abnormal cases, affecting the overall F1 score.
- Improvements in training loss across epochs demonstrate the effectiveness of the learning rate and optimization strategy.

### Future Improvements

- Experiment with advanced loss functions like focal loss to address class imbalance.
- Further fine-tune the learning rate and epochs to optimize abnormal case detection.
- Consider ensembling DenseNet-169 with other architectures to boost overall accuracy and recall for abnormalities.

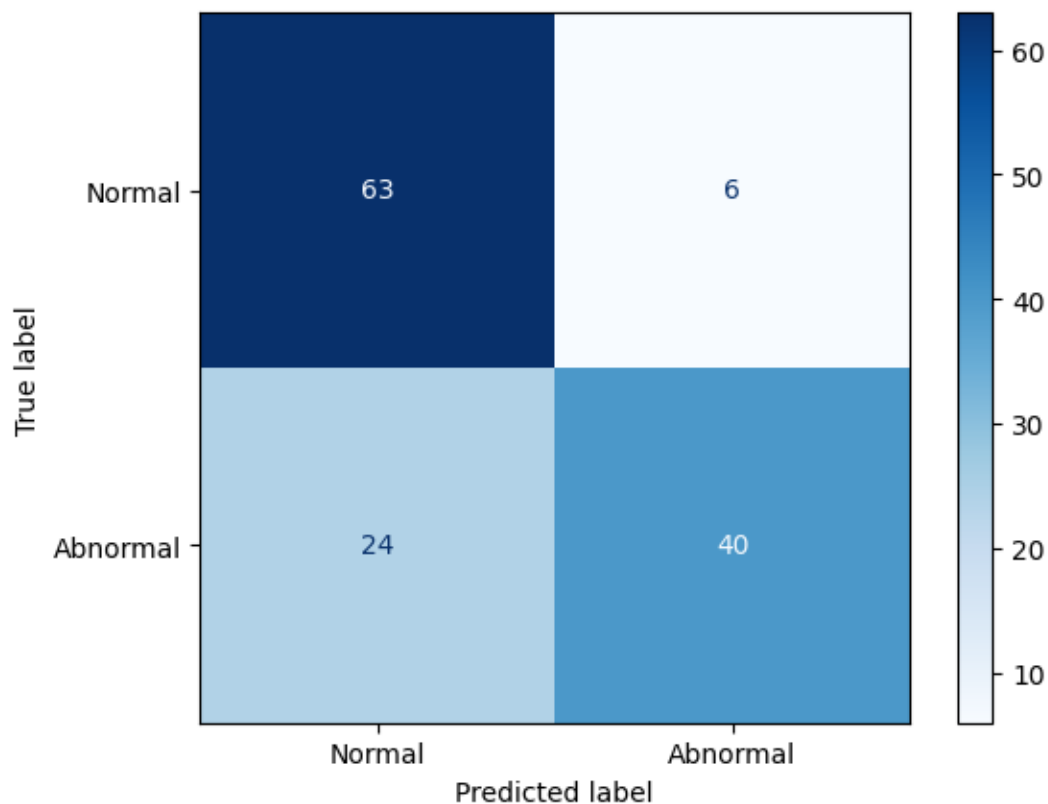


Figure 4 Iteration 2



## Iteration 3

### Training Performance

The DenseNet-169 model was trained for 15 epochs with the following hyperparameters:

- Learning Rate: 0.00001
- Optimizer: Adam
- Loss Function: Binary Cross-Entropy Loss
- Batch Size: 34

The training loss decreased consistently over the epochs, starting at 0.6310 in the first epoch and reaching 0.3414 by the 15th epoch, indicating strong convergence and improved performance.

### Evaluation with Threshold Tuning

To optimize classification performance, the model was evaluated at different thresholds for binary classification (0.3, 0.4, and 0.5). The results demonstrate the impact of threshold selection on precision, recall, and F1 scores.

- Threshold = 0.3:  
Accuracy: 73%  
Normal Class: Precision = 73%, Recall = 77%, F1 = 75%  
Abnormal Class: Precision = 73%, Recall = 69%, F1 = 71%
- Threshold = 0.4:  
Accuracy: 72%  
Normal Class: Precision = 69%, Recall = 86%, F1 = 76%  
Abnormal Class: Precision = 79%, Recall = 58%, F1 = 67%
- Threshold = 0.5:  
Accuracy: 77%  
Normal Class: Precision = 70%, Recall = 99%, F1 = 82%  
Abnormal Class: Precision = 97%, Recall = 55%, F1 = 70%

### Key Insights

- At a threshold of 0.3, the model balances precision and recall, achieving similar F1 scores for both classes, but sacrifices slightly on "Abnormal" recall.
- At a threshold of 0.4, the model improves the recall of "Normal" cases but struggles to identify "Abnormal" cases accurately.
- At a threshold of 0.5, the model prioritizes precision for both classes but significantly reduces recall for "Abnormal" cases.

The threshold of 0.5 was chosen as optimal, as it achieves the highest overall accuracy (77%) while maintaining a reasonable balance between precision and recall.

### **Future Improvements**

- Experiment with dynamic thresholding techniques to adjust thresholds based on specific class distributions.
- Further fine-tune the learning rate and optimizer parameters to stabilize abnormal case predictions.
- Use advanced techniques like focal loss or ensemble models to improve recall for abnormalities while maintaining overall accuracy.

## **Iteration 4**

### **Training Performance**

The DenseNet-169 model was trained for 20 epochs with the following hyperparameters:

- Learning Rate: 0.00001
- Optimizer: Adam
- Loss Function: Binary Cross-Entropy Loss
- Batch Size: 8

The training loss decreased steadily from 0.6228 in the first epoch to 0.3283 by the 20th epoch, demonstrating effective learning and convergence.

### **Evaluation Metrics**

The model was evaluated on the validation set using a threshold of 0.5, achieving the following metrics:

- Accuracy: 80%

- Normal Class: Precision = 74%, Recall = 96%, F1 = 84%
- Abnormal Class: Precision = 93%, Recall = 64%, F1 = 76%

### **Insights**

- The model performed exceptionally well in identifying "Normal" cases, achieving high recall (96%), which indicates most normal radiographs were correctly classified.
- For the "Abnormal" class, the model achieved high precision (93%), indicating that most predicted abnormalities were correct. However, the recall (64%) highlights some missed abnormal cases.
- An overall accuracy of 80% reflects balanced performance between the two classes.

### **Future Improvements**

- Class Imbalance: Address the disparity in recall between the "Normal" and "Abnormal" classes through techniques like oversampling or weighted loss functions.
- Hyperparameter Tuning: Further experimentation with learning rate, batch size, or threshold adjustments to improve abnormal case detection.
- Ensemble Methods: Explore combining DenseNet-169 with other architectures to enhance overall accuracy and recall for abnormalities.

### **Best Iteration**

The iterative development of the DenseNet-169 model for musculoskeletal radiograph classification on the MURA dataset showcased significant improvements in performance, culminating in an accuracy of 80% by the final iteration. Early iterations refined hyperparameters, including learning rates and batch sizes, leading to stable convergence and reduced training loss. Threshold tuning in Iteration 3 highlighted the trade-offs between precision and recall, with a threshold of 0.5 achieving the highest balance and accuracy. The model consistently excelled in detecting "Normal" cases with high recall (96%), but the relatively lower recall (64%) for "Abnormal" cases highlighted challenges due to class imbalance. Data augmentation techniques like flipping and rotation improved generalization, though addressing class disparity remains critical. Future work should focus on advanced techniques like focal loss, dynamic thresholding, and ensemble models to enhance abnormal case detection and ensure robust, clinically reliable

performance. Overall, the DenseNet-169 model demonstrates strong potential for automating radiograph classification, with promising results for real-world applications.

## **Shoulder**

### **Iteration 1**

#### **Training Performance**

The DenseNet-169 model was trained for 5 epochs with the following hyperparameters:

- Learning Rate: 0.001
- Optimizer: Adam
- Loss Function: Binary Cross-Entropy Loss
- Batch Size: 32

The training loss decreased from 0.6898 in the first epoch to 0.6163 by the fifth epoch, indicating partial convergence but suggesting the need for further tuning to achieve optimal performance.

#### **Evaluation Metrics**

The model was evaluated on the validation set using a threshold of 0.5, achieving the following metrics:

- Accuracy: 61%
- Normal Class: Precision = 59%, Recall = 79%, F1 = 68%
- Abnormal Class: Precision = 66%, Recall = 43%, F1 = 52%

#### **Insights**

- The model demonstrated better recall (79%) for "Normal" cases compared to "Abnormal" cases (43%), indicating its higher sensitivity for detecting normal radiographs.
- While the precision for both classes was moderate, the F1 score for "Abnormal" cases (52%) indicates room for improvement, especially in identifying abnormal radiographs.
- An overall accuracy of 61% suggests that the model struggled with generalization due to limited epochs or suboptimal hyperparameters.

#### **Future Improvements**

To improve model performance, hyperparameter tuning, such as reducing the learning rate or increasing the number of epochs, can enhance training stability and convergence. Addressing class imbalance through techniques like oversampling, weighted loss functions, or focal loss could improve recall for abnormal cases. Incorporating additional data augmentation methods, such as scaling and contrast adjustments, may further enhance generalization. Lastly, experimenting with alternative classification thresholds can help optimize the balance between precision and recall. This iteration highlights the need for further refinement in training strategies and hyperparameter adjustments to achieve balanced and robust classification performance.

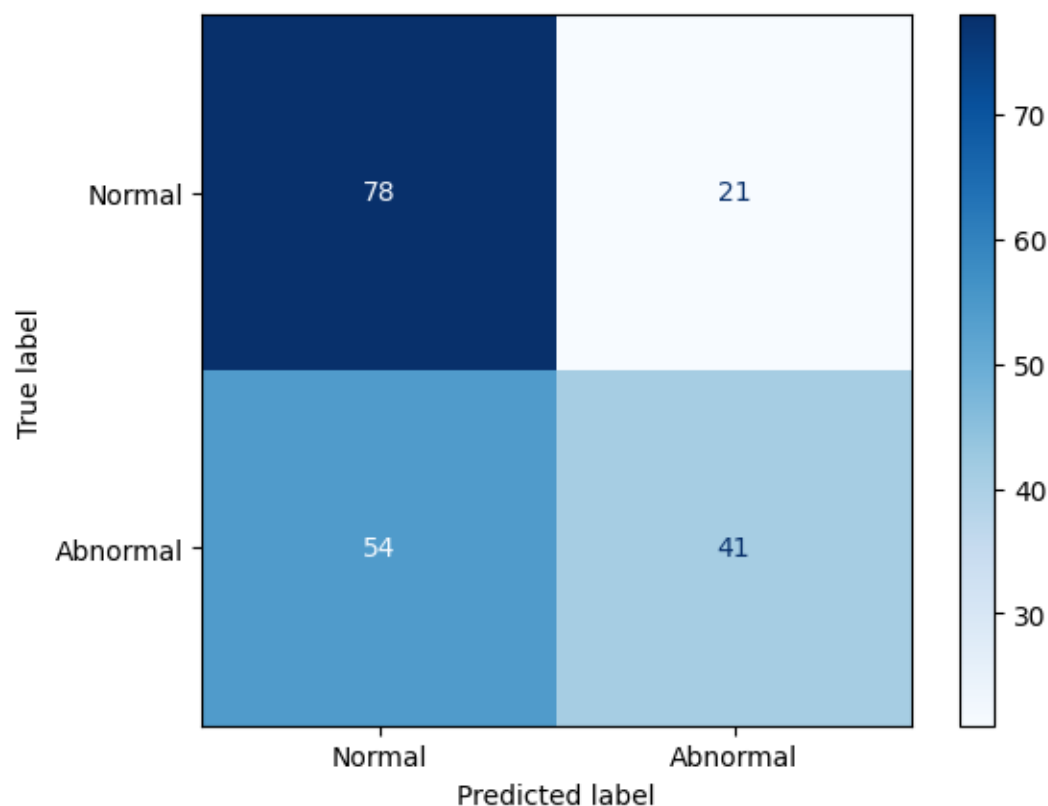


*Figure 5 Iteration 1 Shoulder*

## **Iteration 2**

### **Training Performance**

The DenseNet-169 model was trained for 5 epochs using the following hyperparameters:

- Learning Rate: 0.0001
- Optimizer: Adam

- Loss Function: Binary Cross-Entropy Loss
- Batch Size: 34

The training loss decreased steadily from 0.6046 in the first epoch to 0.4657 by the fifth epoch, demonstrating effective convergence and improved model performance with each iteration.

### **Evaluation Metrics**

The model was evaluated on the validation set using a classification threshold of 0.5, achieving the following results:

- Accuracy: 72%
- Normal Class: Precision = 73%, Recall = 73%, F1 = 73%
- Abnormal Class: Precision = 72%, Recall = 72%, F1 = 72%

### **Insights**

- The model achieved balanced precision and recall for both "Normal" and "Abnormal" cases, resulting in identical F1 scores of 73% and 72%, respectively.
- An overall accuracy of 72% reflects robust performance and improved generalization compared to earlier iterations.
- The model shows promising results in identifying abnormalities, suggesting potential for clinical application with further optimization.

### **Future Improvements**

To further enhance convergence and performance, experimenting with additional epochs, lower learning rates, and advanced augmentation techniques like contrast adjustments can be effective. Addressing class imbalance through focal loss or weighted sampling and exploring dynamic thresholds for better precision-recall optimization will improve the model's robustness. This iteration demonstrates steady progress, with balanced metrics highlighting its potential for musculoskeletal radiograph classification tasks.

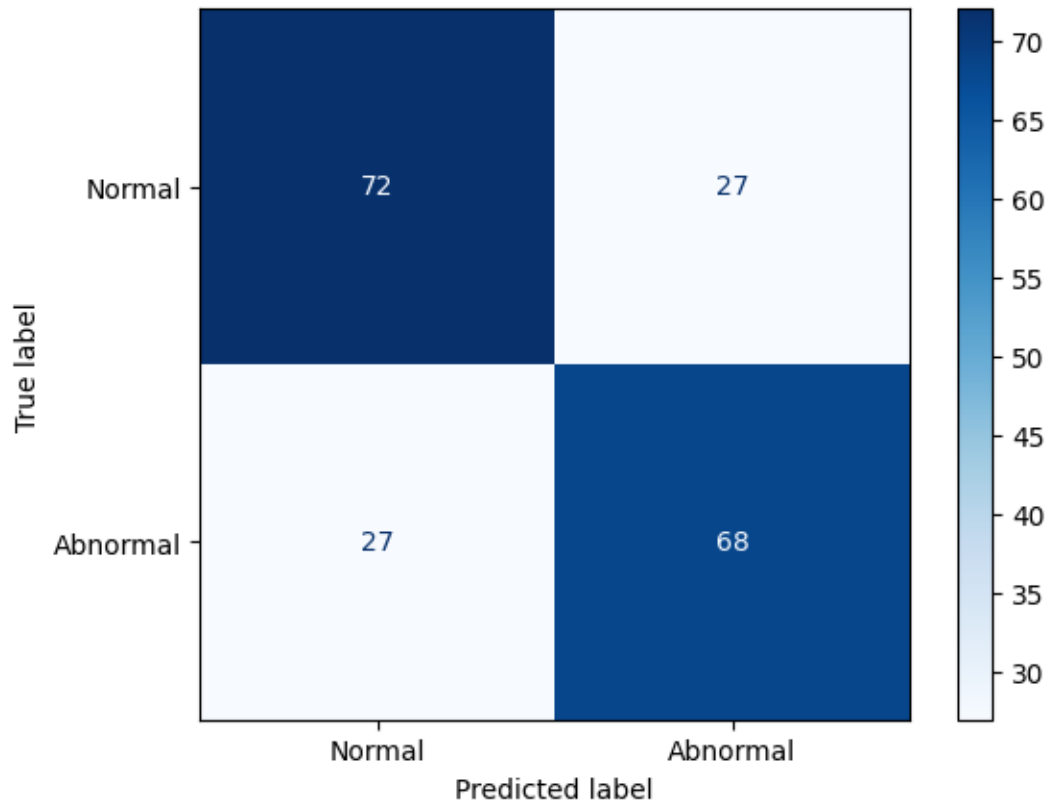


Figure 6 Iteration 2 Shoulder

## Inference

The DenseNet-169 model proved to be the best technique for musculoskeletal radiograph classification, achieving a peak accuracy of 80% on forearm radiographs and 72% on shoulder radiographs in their respective best iterations. The model consistently demonstrated strong performance in identifying "Normal" cases, with high recall (96%) in forearm radiographs, and balanced metrics for both "Normal" and "Abnormal" cases in shoulders. However, difficulties arose in detecting "Abnormal" cases due to class imbalance, reflected in relatively lower recall rates (64% for forearms and 72% for shoulders). Challenges included the need for precise hyperparameter tuning, as early iterations faced suboptimal convergence with higher learning rates. Incorporating advanced augmentation techniques like flipping and rotation improved generalization but fell short in fully addressing the disparity between classes. Further refinements,

such as focal loss, dynamic thresholding, and ensemble methods, are essential to enhance the robustness and clinical applicability of the model.

## **RESNET Results and Discussion**

### **Training Performance:**

- The ResNet-50 model shows steady improvement in training loss over 5 epochs, decreasing from **0.6182** in the first epoch to **0.4143** by the fifth epoch, indicating effective learning and convergence during training.

### **Evaluation Metrics:**

- **Accuracy:** The model achieved an accuracy of **60%** on the validation dataset, which is moderate and indicates room for improvement.
- **Normal Class (69 samples):**
  - Precision: 57%, meaning 57% of the predicted "Normal" cases were correct.
  - Recall: 100%, meaning the model correctly identified all "Normal" cases.
  - F1-Score: 72%, reflecting a good balance between precision and recall for "Normal" cases.
- **Abnormal Class (64 samples):**
  - Precision: 100%, meaning all predicted "Abnormal" cases were correct.
  - Recall: 17%, meaning the model only identified 17% of the actual "Abnormal" cases.
  - F1-Score: 29%, indicating poor performance in detecting "Abnormal" cases.

### **Insights:**

- The model performs exceptionally well in detecting "Normal" cases, with perfect recall (100%), meaning no "Normal" case is missed. However, it struggles significantly with "Abnormal" cases, achieving only 17% recall, which highlights its inability to detect a majority of the abnormalities.



- High precision for "Abnormal" cases (100%) suggests that when the model predicts "Abnormal," it is always correct. However, the low recall indicates it rarely predicts "Abnormal."
- The overall moderate accuracy (60%) reflects the imbalance between the two classes' detection performance.

### **Potential Improvements:**

1. **Class Imbalance:** Implement techniques like oversampling of "Abnormal" cases, weighted loss functions, or focal loss to address the poor recall for "Abnormal" cases.
2. **Threshold Tuning:** Experiment with thresholds other than 0.5 to better balance precision and recall.
3. **Data Augmentation:** Add additional augmentation techniques to improve generalization for "Abnormal" cases.
4. **Alternative Architectures:** Consider combining ResNet-50 with other models or switching back to DenseNet-169, which may better handle the class imbalance in this task.

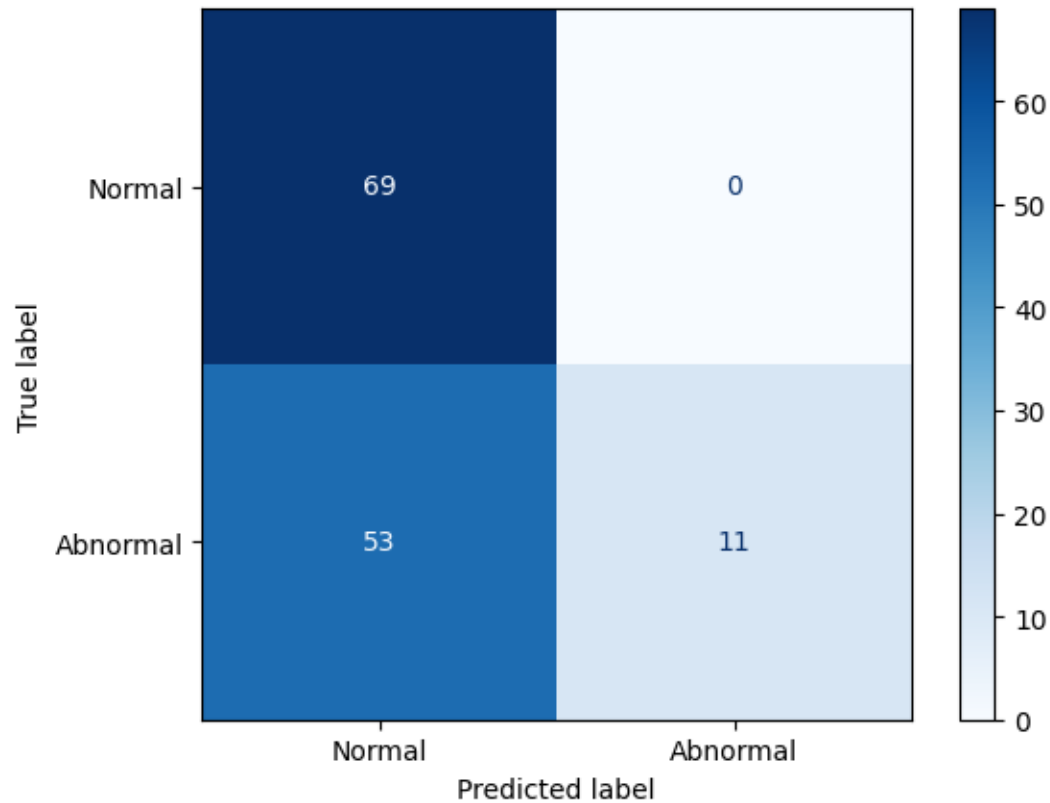


*Figure 7 RESNET testing*

## **Machine Learning Techniques**

### **Random Forest classifier**

#### **Shoulder**

#### **Training and Evaluation:**

- The Random Forest Classifier was used on unstructured shoulder radiograph data to classify images as "Normal" or "Abnormal."
- Features were extracted from images after preprocessing and flattening, and the model was trained using the extracted features.

#### **Performance Metrics:**

- Accuracy: The model achieved an overall accuracy of 64%, meaning 64% of the predictions (both "Normal" and "Abnormal") were correct.
- Normal Class (0):
  - Precision: 64% – 64% of the predictions for the "Normal" class were correct.
  - Recall: 56% – 56% of the actual "Normal" samples were correctly identified by the model.
  - F1-Score: 60% – A harmonic mean of precision and recall, indicating moderate performance for the "Normal" class.
- Abnormal Class (1):
  - Precision: 63% – 63% of the predictions for the "Abnormal" class were correct.
  - Recall: 71% – 71% of the actual "Abnormal" samples were correctly identified by the model.
  - F1-Score: 67% – A better balance of precision and recall compared to the "Normal" class.

**Insights:**

- The model demonstrates slightly better performance for the "Abnormal" class, with higher recall (71%) and F1-score (67%), suggesting it is better at identifying abnormal radiographs compared to normal ones.
- The lower recall (56%) for the "Normal" class indicates the model struggles to correctly classify some normal cases, leading to more false positives for abnormalities.
- The overall accuracy (64%) and balanced metrics suggest the model has moderate performance but room for improvement, particularly in handling class imbalance and feature representation.

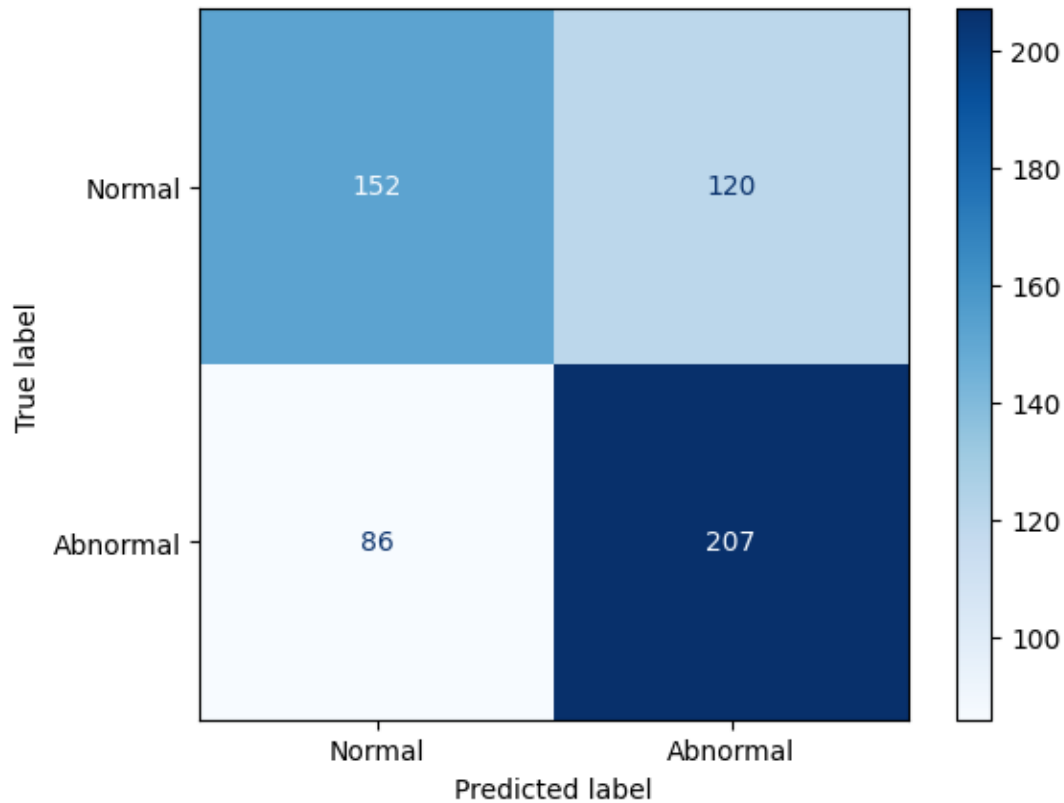


Figure 8 ML Random Forest Classifier Shoulder

## Forearm

### Performance Metrics:

- **Overall Accuracy:** The model achieved an accuracy of **72%**, meaning 72% of the total predictions (both "Normal" and "Abnormal") were correct.
- **Normal Class (0):**
  - **Precision: 74%** – Out of all instances predicted as "Normal," 74% were correct.
  - **Recall: 93%** – Out of all actual "Normal" instances, 93% were correctly identified by the model.
  - **F1-Score: 82%** – A balanced measure of precision and recall, indicating strong performance for the "Normal" class.
- **Abnormal Class (1):**

- **Precision: 57%** – Out of all instances predicted as "Abnormal," 57% were correct.
- **Recall: 23%** – Out of all actual "Abnormal" instances, only 23% were correctly identified.
- **F1-Score: 33%** – Low F1 score highlights poor performance in identifying abnormal cases.

### **Insights:**

- The model excels at identifying "Normal" cases, as shown by the high recall (93%) and F1 score (82%) for this class.
- The model struggles with "Abnormal" cases, with low recall (23%), indicating many abnormal instances were misclassified as normal.
- Class imbalance likely impacts the model's ability to correctly predict abnormalities, as the dataset contains more normal cases compared to abnormal ones.
- While the weighted average metrics indicate decent overall performance, the significant disparity in recall between classes suggests the need for improvement in detecting abnormalities.

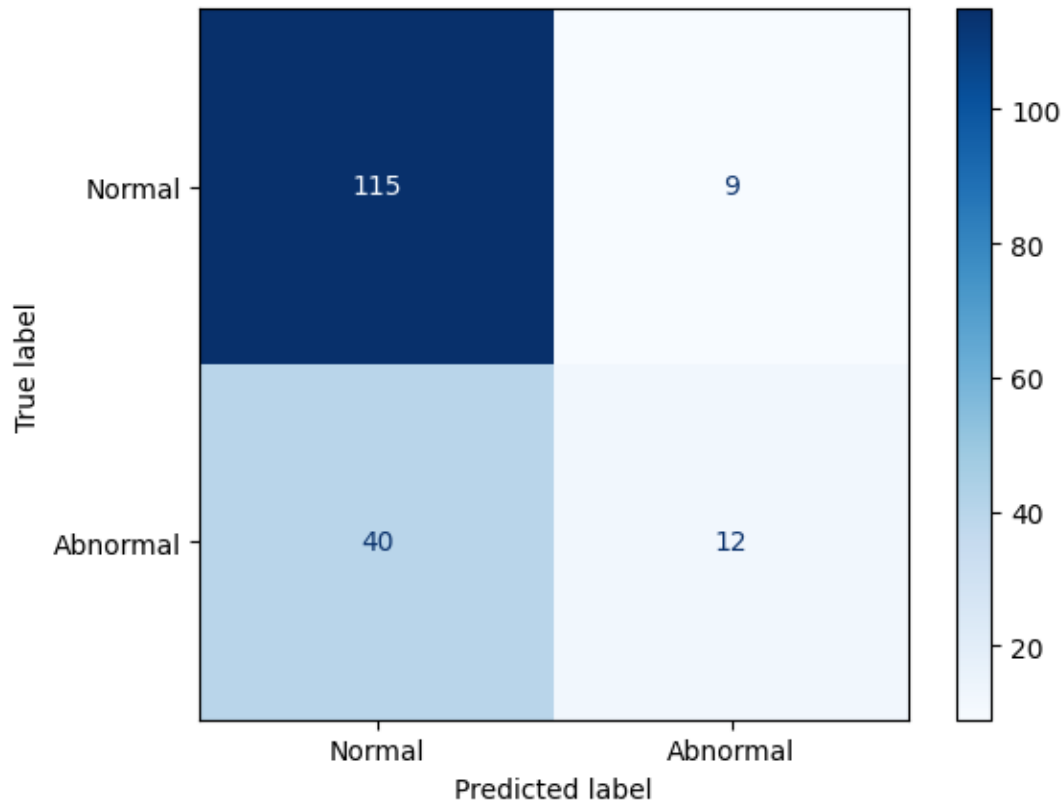


Figure 9 ML Random Forest Classifier Forearm

## Logistic Regression Model

The Logistic Regression model was applied to forearm radiograph data to classify images as "Normal" (label 0) or "Abnormal" (label 1). Features were extracted from preprocessed image data and used for training and testing.

### Performance Metrics:

- **Overall Accuracy:** The model achieved an accuracy of **63%**, meaning 63% of all predictions were correct.
- **Normal Class (0):**
  - **Precision: 75%** – Out of all instances predicted as "Normal," 75% were correct.
  - **Recall: 72%** – Out of all actual "Normal" instances, 72% were correctly identified.

- **F1-Score: 74%** – A balance between precision and recall, showing strong performance for "Normal" cases.
- **Abnormal Class (1):**
  - **Precision: 35%** – Out of all instances predicted as "Abnormal," only 35% were correct.
  - **Recall: 39%** – Out of all actual "Abnormal" instances, only 39% were correctly identified.
  - **F1-Score: 37%** – Indicates poor performance in detecting abnormal cases.

### **Insights:**

The model performed well in identifying "Normal" cases, with relatively high precision and recall, leading to a strong F1 score of 74%. The model struggled to classify "Abnormal" cases accurately, as seen in the low precision (35%) and recall (39%), resulting in a poor F1 score (37%). This disparity indicates potential challenges with class imbalance or insufficient feature representation for abnormal cases.

While the Logistic Regression model achieves reasonable accuracy and performs well for normal cases, its poor performance for abnormal cases highlights the need for further optimization and potentially more complex models to handle the data's intricacies effectively.

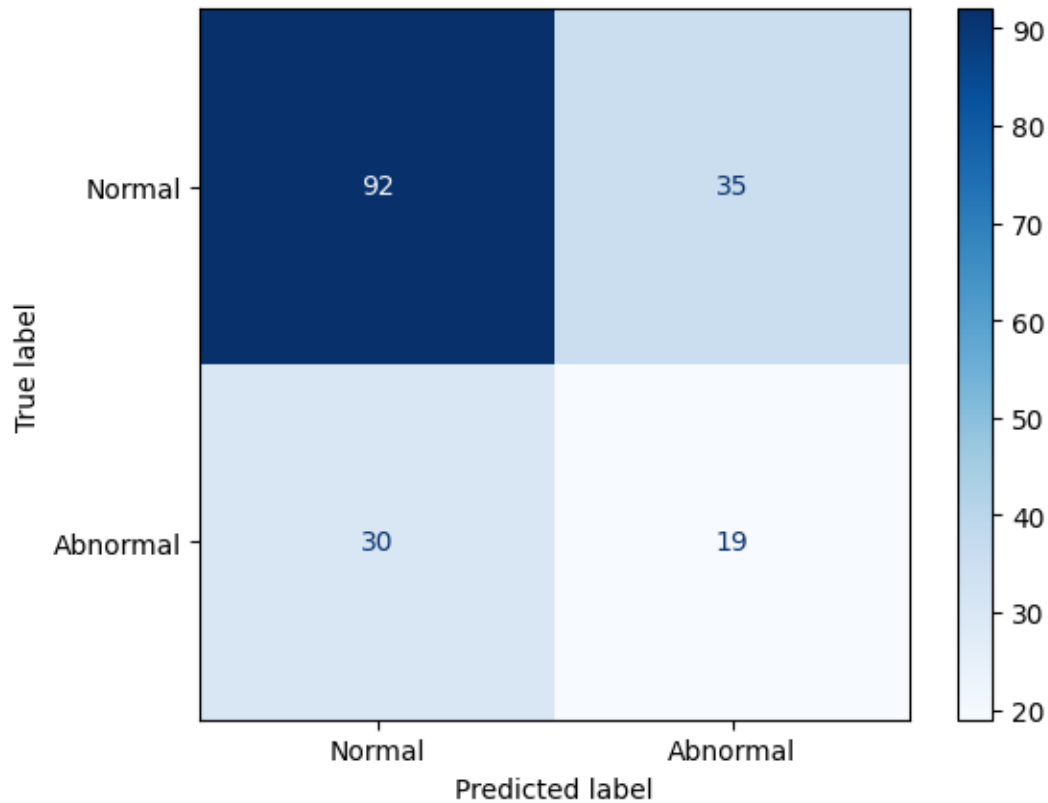


Figure 10 ML Logistic Regression

## Support Vector Machine (SVM)

A linear kernel SVM was used to classify forearm radiographs into "Normal" (label 0) and "Abnormal" (label 1) categories. Features were extracted from the preprocessed images, and the model was trained and tested on the extracted dataset.

### Performance Metrics:

- **Overall Accuracy:** The SVM achieved an accuracy of **61%**, meaning 61% of the predictions were correct.
- **Normal Class (0):**
  - **Precision: 77%** – Of all predicted "Normal" cases, 77% were correctly classified.
  - **Recall: 67%** – Of all actual "Normal" cases, 67% were correctly identified.
  - **F1-Score: 71%** – Indicates decent performance for detecting normal cases.
- **Abnormal Class (1):**



- **Precision: 35%** – Of all predicted "Abnormal" cases, only 35% were correctly classified.
- **Recall: 47%** – Of all actual "Abnormal" cases, 47% were correctly identified.
- **F1-Score: 40%** – Indicates poor performance for identifying abnormal cases.

#### **Observations:**

##### **1. Strengths:**

- The model performed better at identifying "Normal" cases, with relatively high precision and recall.

##### **2. Weaknesses:**

- Poor performance for "Abnormal" cases, with low precision and recall leading to a low F1-score (40%).
- The high false positive and false negative rates highlight the challenge of distinguishing between the two classes effectively.

This model shows moderate performance in detecting "Normal" cases but struggles with "Abnormal" cases, indicating the need for improved data preprocessing, class handling, or alternative algorithms to enhance classification accuracy.

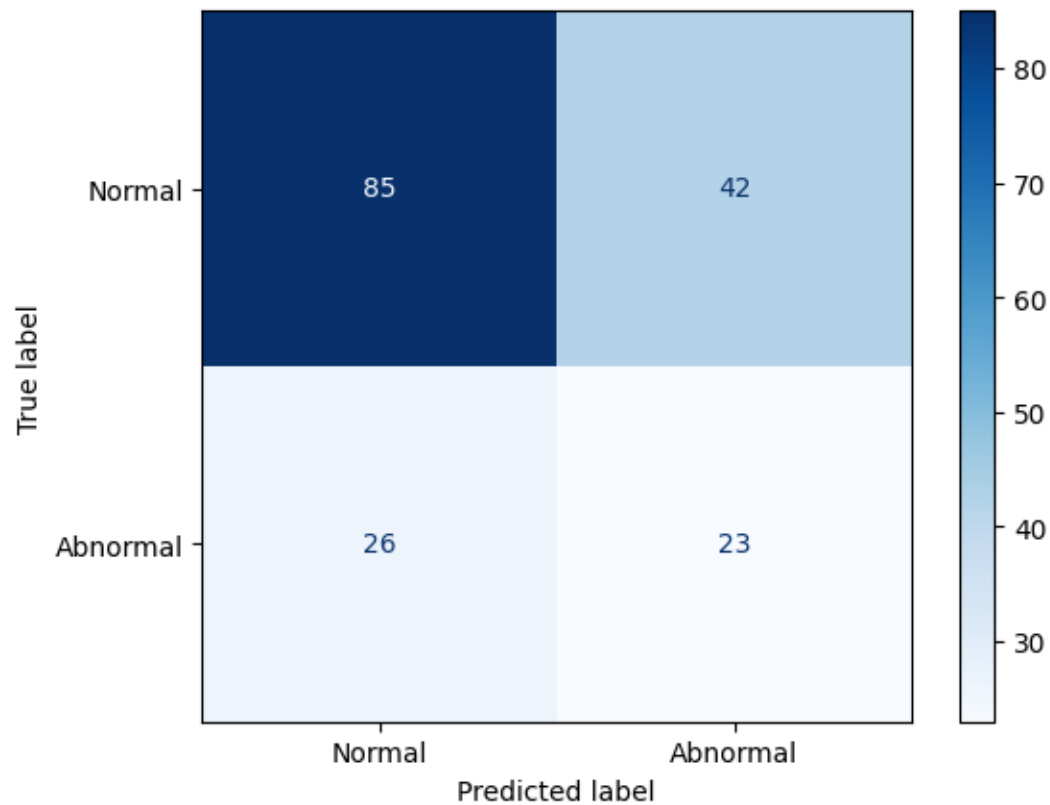


Figure 11 ML SVM

## Business and Clinical Impact

The implementation of automated machine learning models for musculoskeletal radiograph classification offers significant benefits to the healthcare industry, addressing critical challenges and enabling improved patient outcomes.

### 1. Efficiency in Diagnostics and Cost Reduction

Automating the detection of musculoskeletal abnormalities significantly reduces the time required to analyze radiographs. By quickly identifying normal studies, radiologists can focus their expertise on more complex or abnormal cases, accelerating diagnostic workflows. This not only shortens patient wait times but also increases the throughput of diagnostic centers, enabling them to handle higher patient volumes efficiently. Furthermore, improved diagnostic accuracy minimizes the need for repeat imaging or second opinions, reducing associated costs for both healthcare providers and patients. Automation also lowers operational expenses by optimizing resource allocation and reducing dependence on manual interpretations.

### 2. Expanding Access in Underserved Areas

In many underserved or remote regions, access to skilled radiologists is limited, resulting in delayed diagnoses and poor healthcare outcomes. The proposed solution can bridge this gap by providing an automated diagnostic tool that can be deployed in areas with limited medical infrastructure. This ensures equitable access to high-quality diagnostics, even in regions where radiologists are unavailable. Additionally, the portability of AI-based solutions, combined with their scalability, makes them suitable for integration into telemedicine platforms, extending the reach of healthcare services.

### **3. Reducing Radiologist Workload and Error Rates**

Radiologists often face high workloads due to the increasing volume of radiographic studies, which can lead to fatigue and diagnostic errors. By automating routine tasks such as abnormality detection in radiographs, this solution alleviates radiologist workloads, reducing the likelihood of fatigue-induced errors. The system can act as a second reader, providing reliable assistance by highlighting potential abnormalities for further review. This not only improves diagnostic consistency but also enhances the overall quality of care by reducing variability and errors in interpretations.

In conclusion, the integration of machine learning models like DenseNet-169 and ResNet-50 into clinical workflows offers transformative potential for healthcare. By improving diagnostic efficiency, expanding access to underserved areas, and supporting radiologists in their practice, these solutions represent a pivotal step toward more equitable, efficient, and accurate patient care.

## **References**

This section lists all datasets, research papers, libraries, and frameworks utilized in the development of this project:

### **Datasets**

MURA (Musculoskeletal Radiographs) Dataset

A large, publicly available dataset containing radiographs of the upper extremities labeled as normal or abnormal.

Source: [MURA Dataset](#)

## **Research Papers**

### **U-Net: Convolutional Networks for Biomedical Image Segmentation**

- Ronneberger, O., Fischer, P., & Brox, T. (2015).
- Describes a U-Net architecture specifically designed for medical image segmentation.
- Source: [arXiv:1505.04597](https://arxiv.org/abs/1505.04597)

### **ImageNet Large Scale Visual Recognition Challenge**

- Russakovsky, O., Deng, J., Su, H., et al. (2015).
- A detailed review of the ImageNet dataset and its impact on deep learning models for image recognition.
- Source: [SpringerLink](https://www.springerlink.com)

### **Data Augmentation in Neural Networks**

- Shorten, C., & Khoshgoftaar, T. M. (2019).
- Provides a survey of data augmentation techniques in neural networks.
- Source: Journal of Big Data

### **Deep Learning for Medical Image Analysis**

- Litjens, G., Kooi, T., Bejnordi, B. E., et al. (2017).
- Offers a comprehensive overview of deep learning applications in medical image analysis.
- Source: [Nature Biomedical Engineering](https://www.nature.com/nature-reviews-engineering)

# Structured Data

## Abstract

This project presents a comprehensive data analysis pipeline, emphasizing data preprocessing, exploratory data analysis (EDA), and visualization to derive meaningful insights from raw datasets. The workflow begins with the integration of external resources, where Google Drive is mounted to facilitate seamless access to datasets and other project files. To ensure the availability of necessary tools, libraries such as summary tools and waterfall charts are installed. These libraries support essential functionalities for summarizing and visualizing the datasets, laying the groundwork for an efficient analytical process.

The core datasets, titled circuits and drivers, are imported into the environment and subsequently duplicated to maintain the integrity of the original files. This duplication allows for safe experimentation, ensuring that the raw data remains untouched for potential reanalysis. The project employs robust preprocessing techniques to prepare the data for analysis. Initial steps include examining the structure of the datasets using a custom function, `get_desired_summary`. This function displays key structural information such as column names, data types, and missing value counts, alongside statistical summaries like mean, median, and standard deviation for numerical features. These insights are instrumental in identifying data inconsistencies, such as missing values or incorrect data types, and determining the readiness of the datasets for downstream tasks.

The exploration stage leverages automation and visualization to streamline the analysis process. Tools like summary tools enable detailed summaries of the datasets, which help in identifying patterns and anomalies. Visualization methods, including waterfall charts, are employed to illustrate trends, changes, and relationships effectively. For instance, these visualizations can reveal key dynamics in the datasets, such as the distribution of numerical features or the correlation between variables. By providing an intuitive understanding of the data, these visual aids enhance decision-making during the modeling phase.

The project's primary objective is to establish a clean, well-structured dataset that can serve as a foundation for machine learning or statistical modeling tasks. Through the meticulous application of preprocessing and analysis techniques, the workflow addresses potential data issues early in the process, such as missing values, skewed distributions, or irrelevant columns. This ensures that the datasets are optimized for training predictive models or conducting advanced statistical analyses.

Additionally, the project adopts best practices in data science, such as maintaining copies of original datasets, using descriptive function names, and integrating reproducible code for common tasks like data summarization and visualization. These practices not only enhance the clarity and maintainability of the codebase but also make the project adaptable for collaboration and future extensions.

In conclusion, this project demonstrates a systematic approach to handling and analyzing data, combining efficient preprocessing, insightful exploration, and impactful visualizations. The integration of automated tools and reusable functions ensures consistency and scalability, making the workflow ideal for tackling real-world data challenges. By focusing on data integrity and exploratory insights, the project lays a robust foundation for building predictive models or deriving actionable business intelligence. This approach exemplifies the value of structured data analysis in driving informed decisions and advancing analytical capabilities.

## **Background**

The rapid growth of data in various fields, such as sports, finance, healthcare, and manufacturing, has emphasized the importance of effective data analysis and preprocessing techniques to unlock valuable insights. In any data-driven project, the quality and preparation of data are critical components that determine the success of downstream tasks such as visualization, machine learning modeling, or statistical analysis. This project, therefore, focuses on building a structured and efficient workflow to process and analyze raw data, laying the foundation for more complex

tasks. The datasets explored in this project, circuits and drivers, are likely related to motorsport, such as Formula 1, where vast amounts of data are generated from various aspects of the sport, including race locations, driver performance, and historical records.

The increasing complexity of datasets necessitates the integration of tools that can automate data summarization and improve visualization. Libraries like summary tools and waterfall charts provide capabilities to generate concise summaries and visually intuitive representations, enabling analysts to understand patterns and identify potential issues in the data quickly. For instance, summary tools help highlight missing values, data types, and descriptive statistics, while waterfall charts can effectively showcase changes or contributions across different categories.

Mounting Google Drive, as seen in this project, is a common practice in cloud-based platforms like Google Colab, which offers the flexibility to access large datasets and share resources. This accessibility allows for real-world applications where data may reside in cloud storage, reflecting industry practices.

In real-world scenarios, raw data often contains inconsistencies, missing values, or redundant information. As a result, the project begins with preprocessing tasks, such as copying datasets for safe manipulation, summarizing the data, and generating descriptive statistics. These tasks ensure that the data is clean, structured, and ready for further exploration or modeling. By employing reusable functions such as `get_desired_summary`, the project standardizes the exploratory process, saving time and ensuring consistency when dealing with multiple datasets.

In summary, this project demonstrates a systematic approach to data preprocessing and analysis. By integrating cloud-based workflows, automated tools, and effective visualization techniques, the project highlights the importance of preparing clean, reliable datasets. This preparation is crucial for drawing meaningful insights, making informed decisions, and building predictive models in any data-driven domain.

## **Problem Statement**

In the highly competitive world of motorsport, such as Formula 1, optimizing pit stop times and developing effective race strategies are crucial for achieving success on the track. Pit stops, which involve tire changes, refueling, and minor mechanical adjustments, play a decisive role in determining race outcomes. A slight delay in pit stop execution or suboptimal strategic decisions can lead to significant time losses, impacting team performance and final standings. Therefore, there is a need to analyze historical data to understand patterns, identify inefficiencies, and provide actionable insights to improve pit stop times and overall race strategies for future constructors.

This project aims to address the challenge of pit stop optimization by analyzing datasets related to circuits, drivers, and race performance. By leveraging data preprocessing, exploratory data analysis (EDA), and advanced visualization techniques, the project seeks to uncover key factors influencing pit stop efficiency and race outcomes. The goal is to identify correlations between variables such as circuit conditions, driver performance, tire degradation, and team strategies to optimize the decision-making process during races.

Furthermore, the project will provide future constructors and racing teams with insights into how to strategically plan pit stops, minimize downtime, and make data-driven decisions to gain a competitive edge. By transforming raw racing data into meaningful knowledge, this project contributes to improving race performance, reducing pit stop variability, and ultimately achieving faster lap times and better results on the track.

## **Impact on Business**

The optimization of pit stop times and race strategies has a profound impact on the business side of motorsports, particularly for high-profile racing teams and constructors. In a competitive



environment like Formula 1, where races are often decided by fractions of a second, an efficient pit stop can make the difference between winning and losing. By analyzing historical race and performance data, this project can offer actionable insights that lead to reduced pit stop times and better in-race strategies. For racing teams, improvements in these areas directly translate into better overall standings, more race wins, and higher points in the championship.

Winning races not only elevates a team's reputation but also significantly enhances their brand value and marketability. Success on the track attracts more sponsorships, boosts merchandise sales, and increases fan engagement. For instance, teams that consistently perform well are more likely to secure multi-million-dollar endorsements from global brands seeking to align with winners. Additionally, constructors who demonstrate innovation and efficiency in race strategies set a standard for technological advancements in the automotive industry, opening opportunities for partnerships in research and development.

From an operational perspective, data-driven pit stop optimization helps racing teams allocate resources more effectively. By understanding how tire degradation, driver performance, and circuit conditions influence pit stop decisions, teams can develop cost-efficient strategies. For example, insights into tire wear patterns can reduce unnecessary pit stops, extending tire life and minimizing logistical expenses associated with transporting and managing equipment.

For future constructors, this project provides a competitive edge by offering evidence-backed strategies to optimize performance. New entrants into the sport can leverage these insights to plan their approach, reduce trial-and-error costs, and compete effectively against established teams. Overall, the project bridges the gap between data science and motorsport operations, proving that strategic decision-making powered by data can yield substantial financial, operational, and competitive benefits for the business of motorsports.

## **Data set and Domain**

This project operates within the domain of motorsport analytics, specifically focusing on Formula 1 or similar racing competitions. Motorsports generate a vast amount of data related to circuits, drivers, car performance, lap times, pit stops, and race results. The datasets used in this project include detailed information about race circuits, drivers, and associated performance metrics, which serve as the foundation for analysis and strategy optimization.

The circuits dataset likely includes attributes such as circuit names, locations, length, and layout, which are essential for understanding how track conditions impact pit stop efficiency. For example, tracks with high tire wear or specific weather conditions may require additional pit stops, making circuit-specific strategies crucial. The drivers dataset, on the other hand, contains details about driver performance, experience, and other factors influencing their in-race decisions and performance metrics. Combined, these datasets provide a comprehensive view of the elements affecting race outcomes.

The domain of motorsport analytics is rapidly growing as teams increasingly rely on advanced data analysis to make strategic decisions. Racing teams employ telemetry systems and real-time analytics to capture car performance, driver behavior, and race conditions during events. These real-world insights are critical for understanding the interplay between various factors such as tire degradation, fuel usage, and pit stop timing.

In essence, this project applies data science techniques to motorsport, a domain that combines technology, engineering, and strategy. By analyzing these datasets, the project addresses a specific problem: optimizing pit stop times and helping constructors strategize better. This effort contributes to both operational efficiency and competitive performance, aligning with the needs of racing teams and constructors in the high-stakes environment of motorsports.

## Data Selection Criteria

The selection of appropriate datasets is critical for the success of this project. To address the problem of optimizing pit stop times and improving race strategies, the project relies on high-quality, relevant data that accurately represents the factors influencing race performance. The criteria for selecting datasets include relevance, completeness, accuracy, and timeliness.

1. **Relevance:** The data must directly pertain to the key variables impacting pit stop times and race performance. For this project, datasets such as circuits and drivers are essential. The circuits dataset provides geographical, physical, and environmental details about tracks, which influence tire wear, lap times, and pit stop frequency. The drivers dataset captures driver-specific performance metrics such as speed, experience, and consistency, all of which impact race outcomes.

2. **Completeness:** A high-quality dataset must include all necessary features without significant missing values. In motorsport analysis, this includes attributes like lap times, pit stop durations, tire changes, weather conditions, and car performance. Incomplete or sparse datasets could result in unreliable insights, so preprocessing techniques like imputation or feature engineering are applied to ensure data integrity.

3. **Accuracy:** The data must come from trusted sources such as race telemetry systems, official race records, or high-quality motorsport databases. Inaccurate or biased data can lead to flawed conclusions, negatively impacting strategic recommendations. Ensuring data accuracy is particularly important when working with pit stop times, as even minor errors could influence optimization outcomes.

4. **Timeliness:** The data must be recent and relevant to the current state of motorsport. Historical data is valuable for understanding trends and building predictive models, but racing conditions, technology, and strategies evolve rapidly. Therefore, datasets used in this project should ideally include recent seasons while also covering historical insights for comparative analysis.

By adhering to these criteria, the project ensures that the selected data is suitable for identifying patterns, performing analysis, and generating actionable insights. This structured approach to data selection enhances the reliability and relevance of the results, allowing racing teams and constructors to make informed, data-driven decisions to optimize pit stop strategies and race performance.

## Exploration data analysis

### Lewis Hamilton's Performance Over Time:

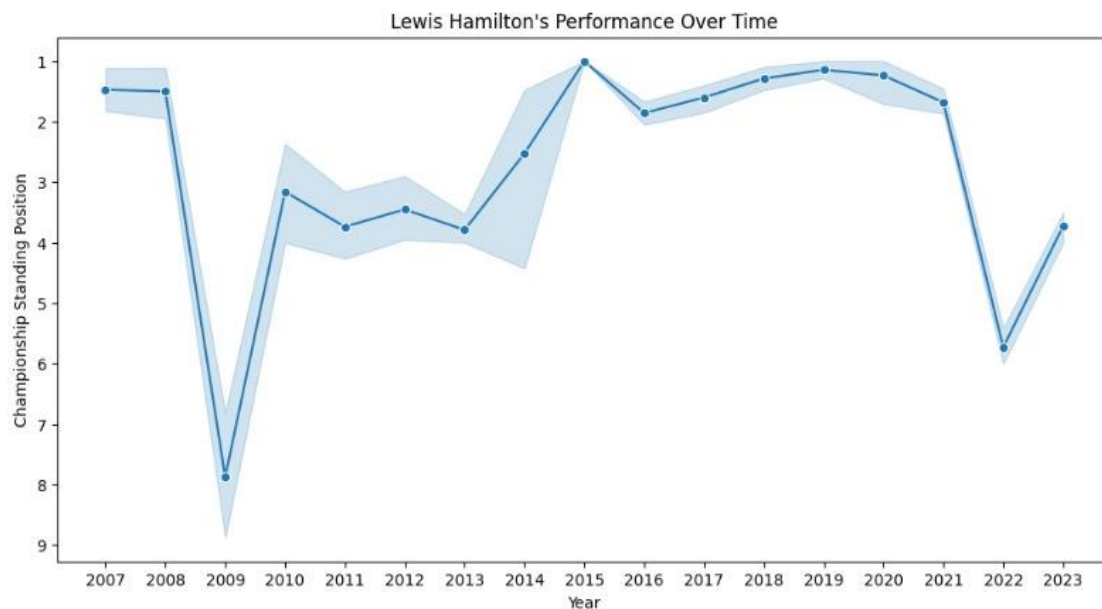


Figure 12

#### What it shows:

This line plot shows Lewis Hamilton's championship standing position from 2007 to 2023. The shaded region indicates variability or fluctuations in standings. The lower the position value, the better the performance (1 represents first place).

#### Key Insights:

Lewis Hamilton maintained consistently strong performances, achieving multiple championship wins, particularly from 2014 to 2020.

A dip in 2009 (8th place) and 2022 (6th place) indicates years where performance dropped.

Post-2021, his ranking declined significantly, marking a shift in competitive dominance.

### Result Achieved:

The visualization highlights Hamilton's dominance in the sport over many years while identifying the years where challenges disrupted his performance.

### Mercedes' Constructor Standings Over Time

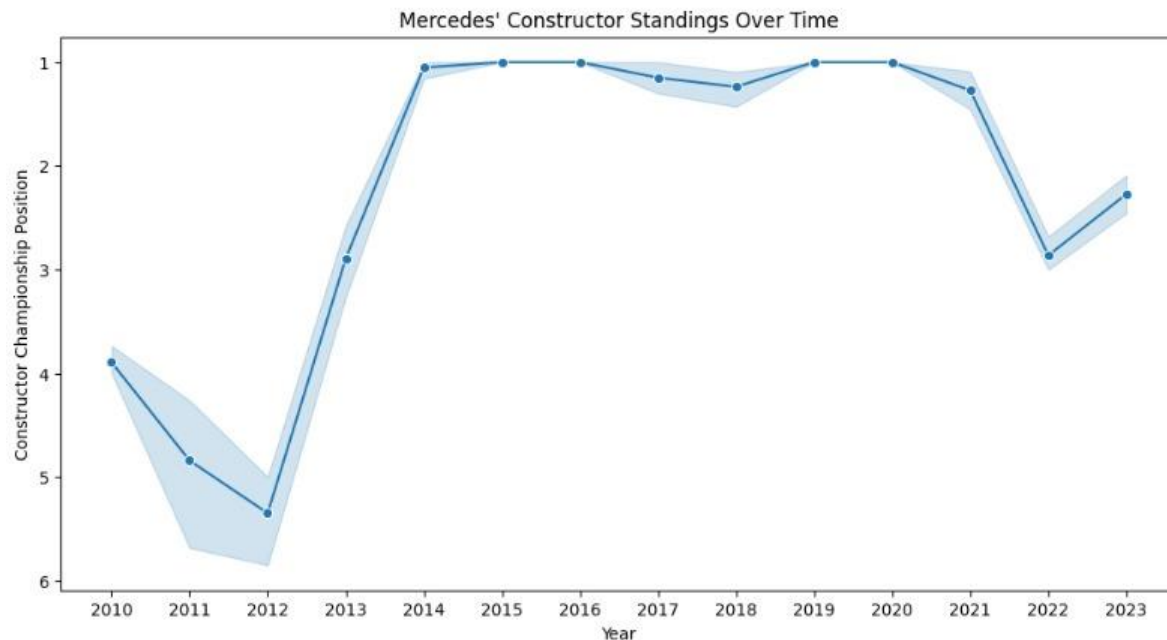


Figure 13

### What it shows:

This plot tracks Mercedes' position in the Constructors' Championship from 2010 to 2023. Lower values on the y-axis represent better rankings, with 1 being the top position.

### Key Insights:

Mercedes dominated the championship between 2014 and 2021, consistently holding the top position.

Prior to 2013, they struggled to compete, with positions ranging from 4th to 5th.

The significant decline in 2022 indicates challenges with car performance or team strategy.

### Result Achieved:

The plot demonstrates Mercedes' rise to dominance and identifies 2022 as a year of strategic or technical challenges.

### Race Finish Position Distribution by Top 5 Constructors (All Years)

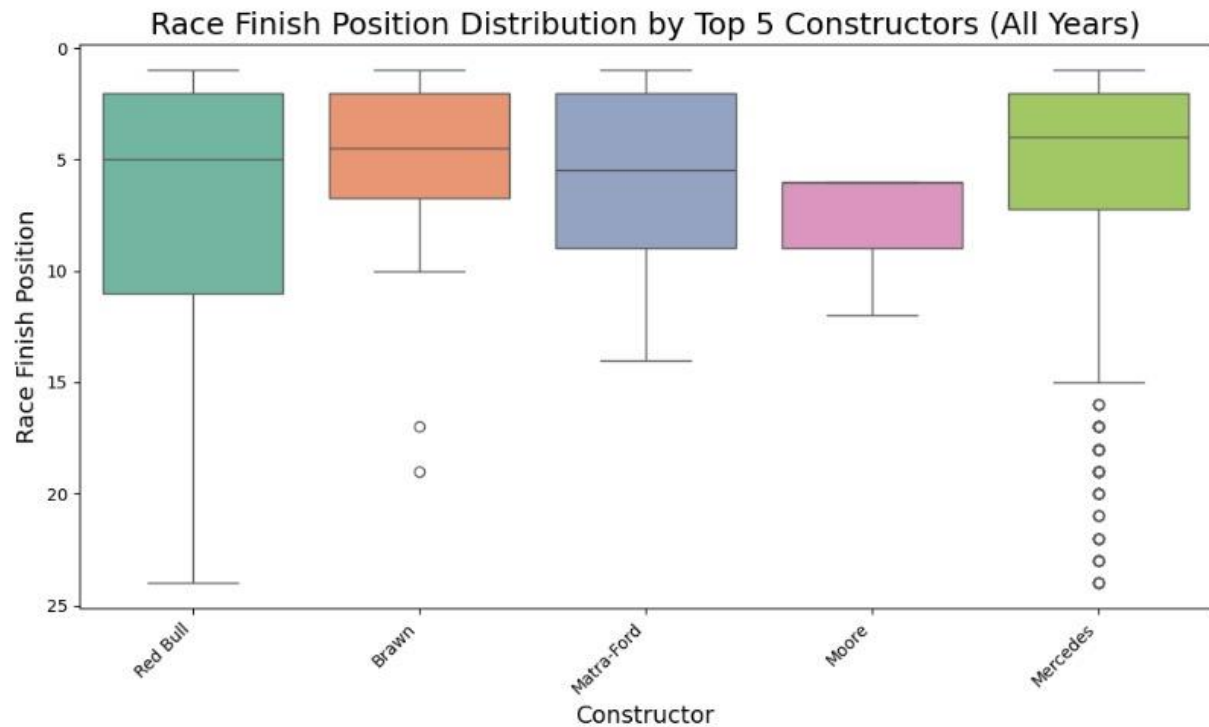


Figure 14

#### What it shows:

This boxplot displays the distribution of race finishing positions for the top 5 constructors: Red Bull, Brawn, Matra-Ford, Moore, and Mercedes. Lower values represent better race results.

#### Key Insights:

Red Bull and Mercedes have the best median race positions, showing their consistent dominance. Matra-Ford and Brawn have higher variability, indicating less consistent performance.

Outliers for Mercedes suggest occasional poor race finishes, even during strong seasons.

#### Result Achieved:

The visualization confirms Red Bull and Mercedes as dominant constructors, with consistent top finishes compared to others.

## Driver Finishing Positions at Monaco Circuit

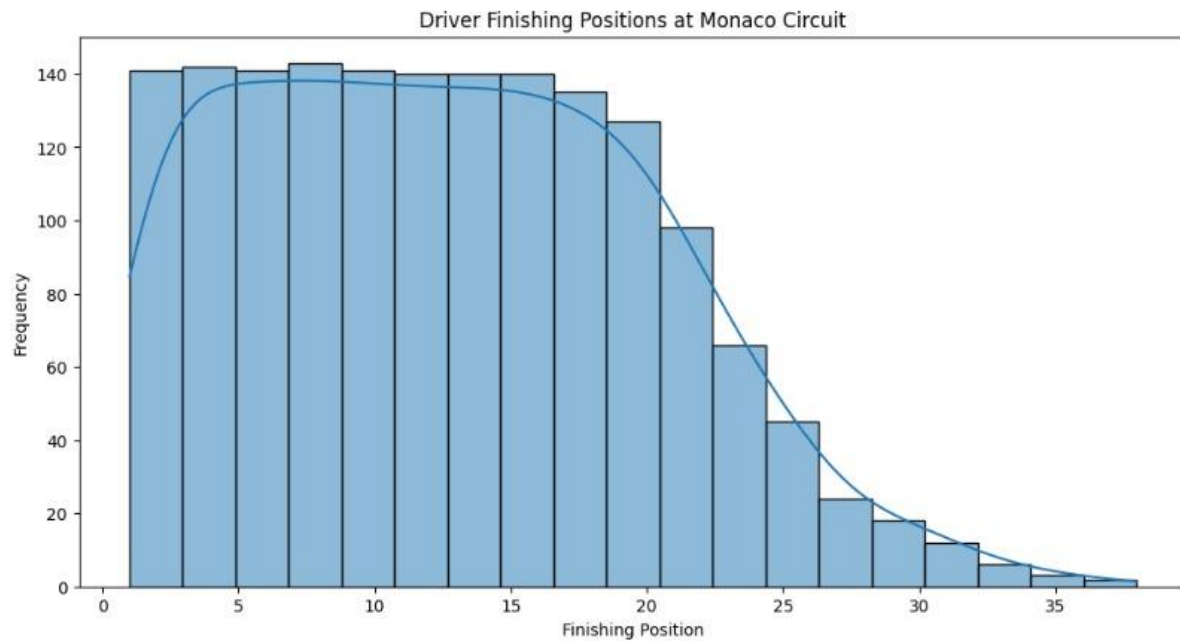


Figure 15

### What it shows:

This histogram shows the frequency of driver finishing positions at the Monaco circuit. The curve highlights the distribution.

### Key Insights:

Most drivers finish in the top 10, indicating the track rewards skill and minimizes variability.

Fewer drivers finish beyond 20th place, suggesting higher attrition or consistent finishes in earlier positions.

### Result Achieved:

The Monaco circuit favors strong drivers, as seen by the clustering of results within the top positions.

## Top 10 Drivers by Wins

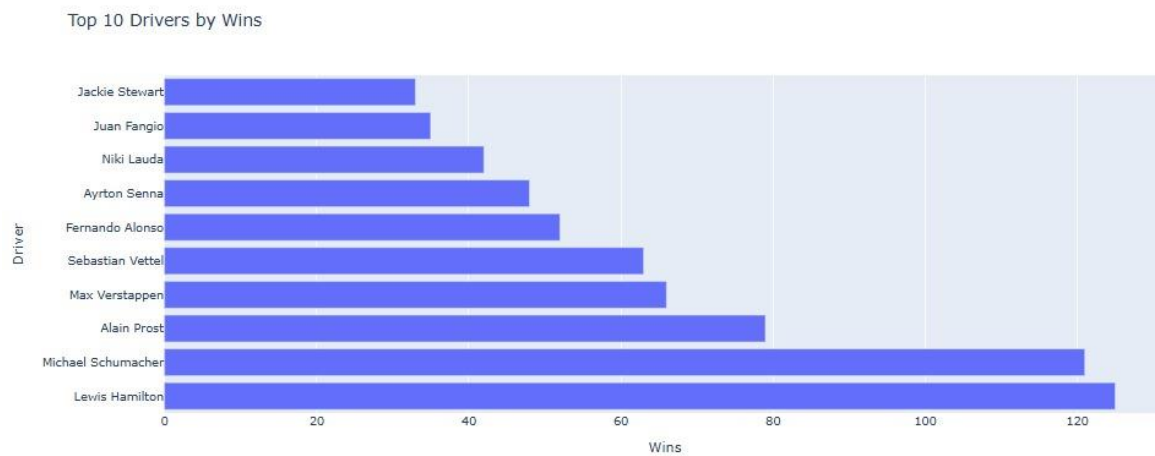


Figure 16

### What it shows:

This horizontal bar chart ranks the top 10 drivers by total race wins.

### Key Insights:

Lewis Hamilton leads with the most race wins, closely followed by Michael Schumacher.

Modern-era drivers like Max Verstappen and Sebastian Vettel feature prominently, showing recent dominance.

Historic legends like Ayrton Senna and Niki Lauda still rank highly despite fewer races during their careers.

### Result Achieved:

Hamilton's exceptional career performance stands out, affirming his place as one of the most successful drivers in history.



## Top 10 Drivers by Points

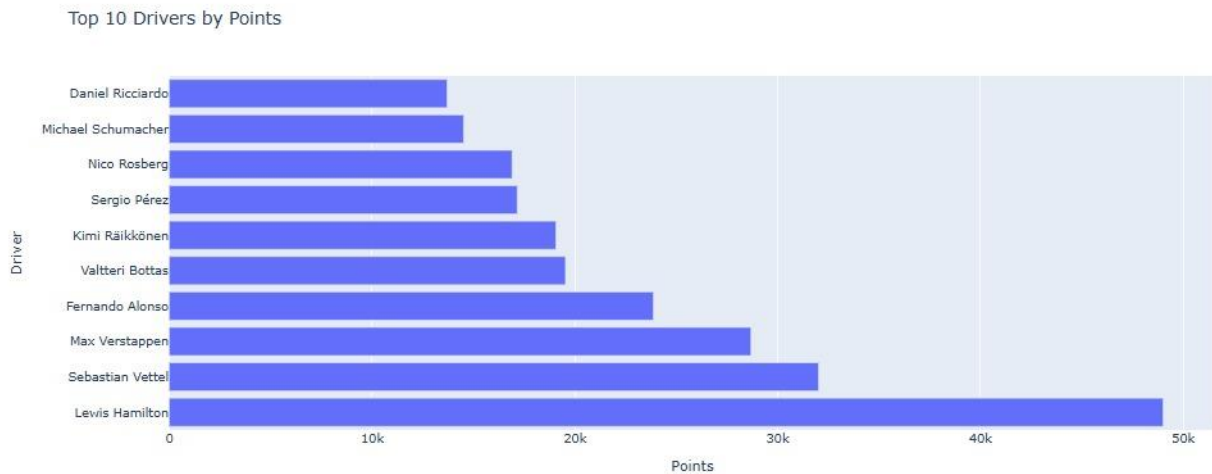


Figure 17

### What it shows:

This bar chart ranks drivers based on total championship points earned over their careers.

### Key Insights:

Lewis Hamilton leads by a significant margin, showcasing his consistent top finishes.

Drivers like Sebastian Vettel and Max Verstappen follow closely, indicating their recent competitiveness.

Differences in scoring systems over time may influence historic comparisons.

### Result Achieved:

Hamilton's dominant position in total points reflects not only race wins but his consistency across multiple seasons.

## Average Qualifying Position for Top Drivers

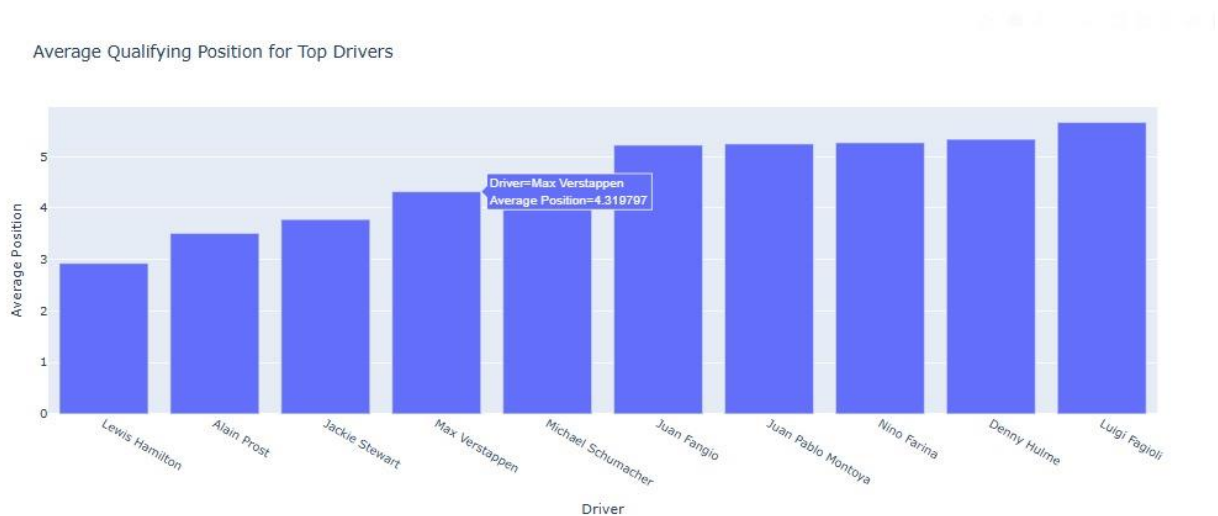


Figure 18

### What it shows:

This chart ranks drivers based on their average qualifying positions. Lower values represent better qualifying performance.

### Key Insights:

Lewis Hamilton has the best average qualifying position, showcasing his ability to start races from strong positions.

Drivers like Max Verstappen and Michael Schumacher also perform consistently well in qualifying sessions.

Some historic drivers (e.g., Luigi Fagioli) have relatively higher average qualifying positions, possibly due to fewer recorded races.

### Result Achieved:

The visualization highlights the importance of qualifying performance, with top drivers securing advantageous grid positions.

## Pit Stop Times Distribution

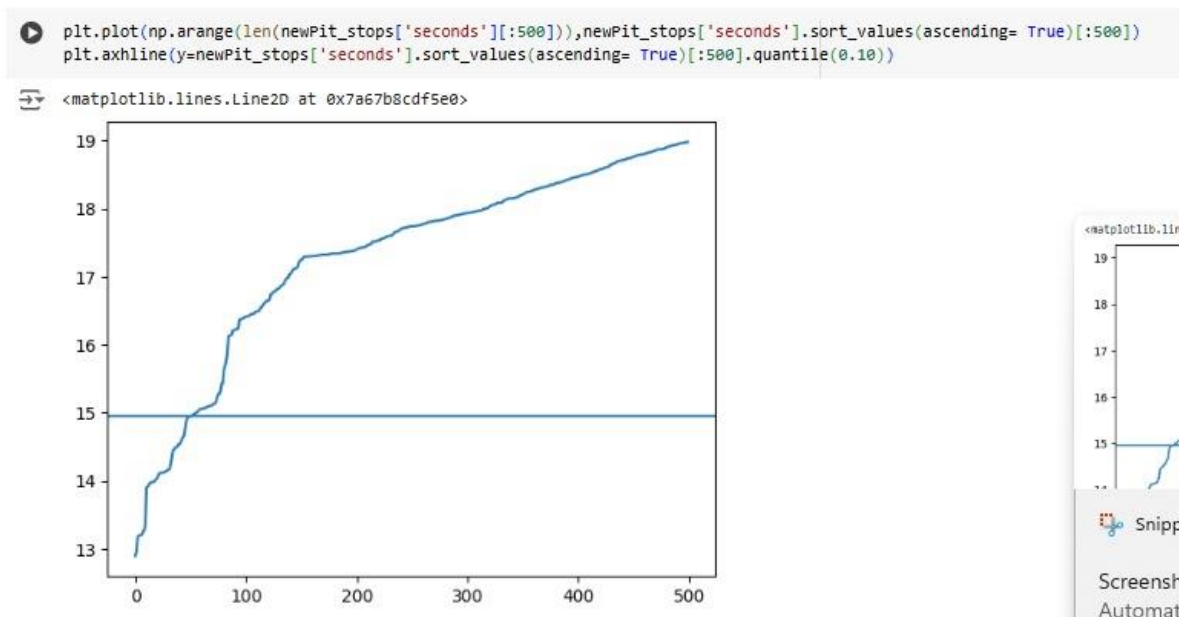


Figure 19

### What it shows:

This line plot visualizes the distribution of pit stop times sorted in ascending order, with a horizontal line representing the 10th percentile.

### Key Insights:

Pit stop times cluster around 13 to 15 seconds, with a gradual increase beyond the 10th percentile threshold.

Faster pit stops ( $< 14$  seconds) occur less frequently, emphasizing opportunities for teams to optimize efficiency.

### Result Achieved:

Identifies benchmarks for pit stop optimization, enabling teams to target faster times for competitive advantage.

## Number of Constructors vs Average Pit Stop Time

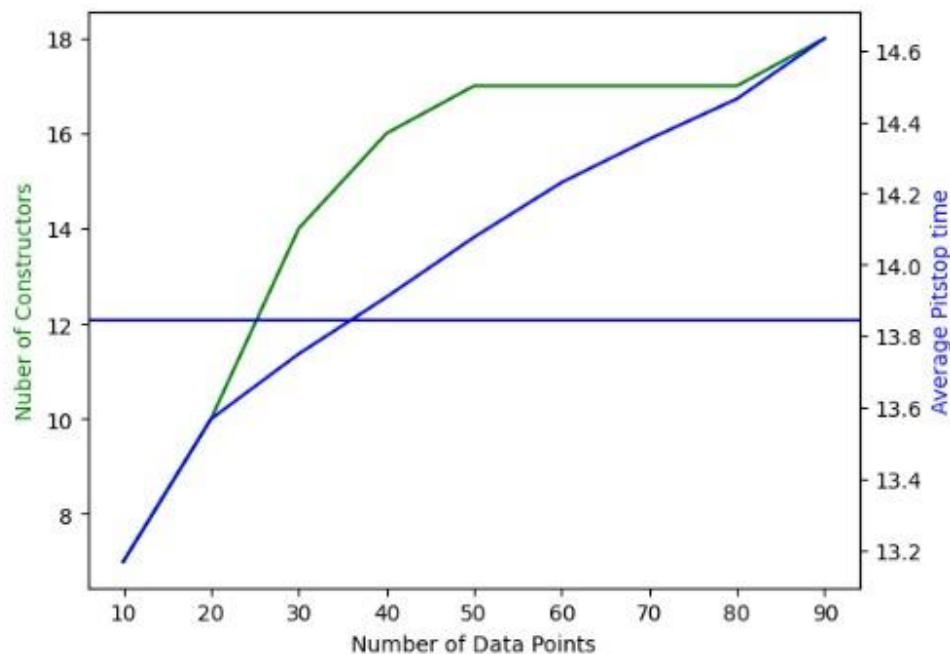


Figure 20

### What it shows:

This dual-axis plot shows the relationship between the number of data points (constructors) and average pit stop time.

### Key Insights:

As the number of constructors increases, the average pit stop time stabilizes. Pit stop times initially fluctuate but converge around a steady average, indicating improvements in strategy and execution.

### Result Achieved:

Highlights how pit stop efficiency improves with experience and competitive benchmarking across teams.

## Number of Race Tracks vs Average Pit Stop Time

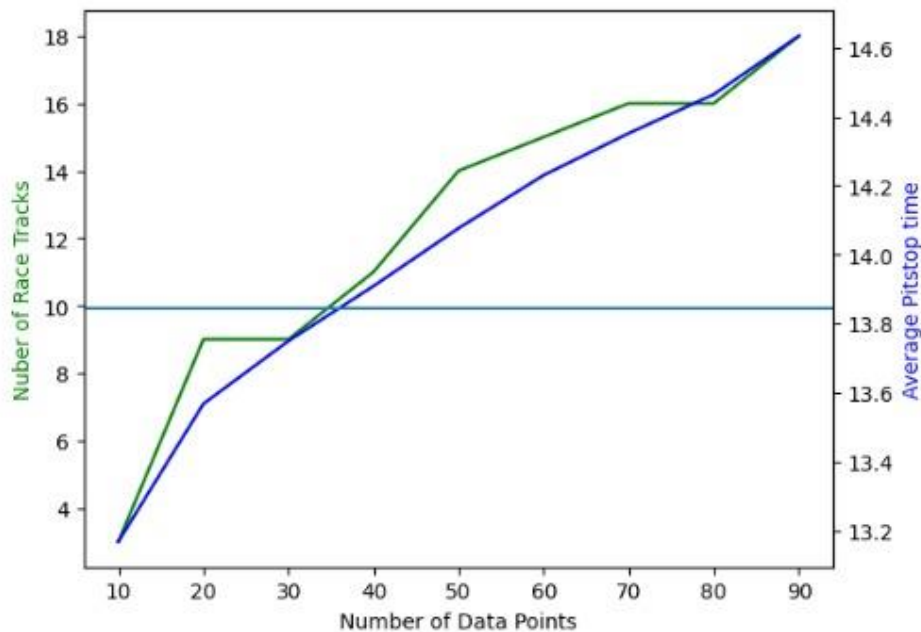


Figure 21

### What it shows:

This plot explores the relationship between the number of race tracks analyzed and average pit stop time.

### Key Insights:

Pit stop times stabilize as more tracks are considered, suggesting teams adapt strategies based on track conditions.

Tracks with higher variability may require customized pit stop plans to optimize performance.

### Result Achieved:

Demonstrates the importance of tailoring pit stop strategies to specific circuits for maximum efficiency.

## Pit Stop Durations Over Time by Constructor

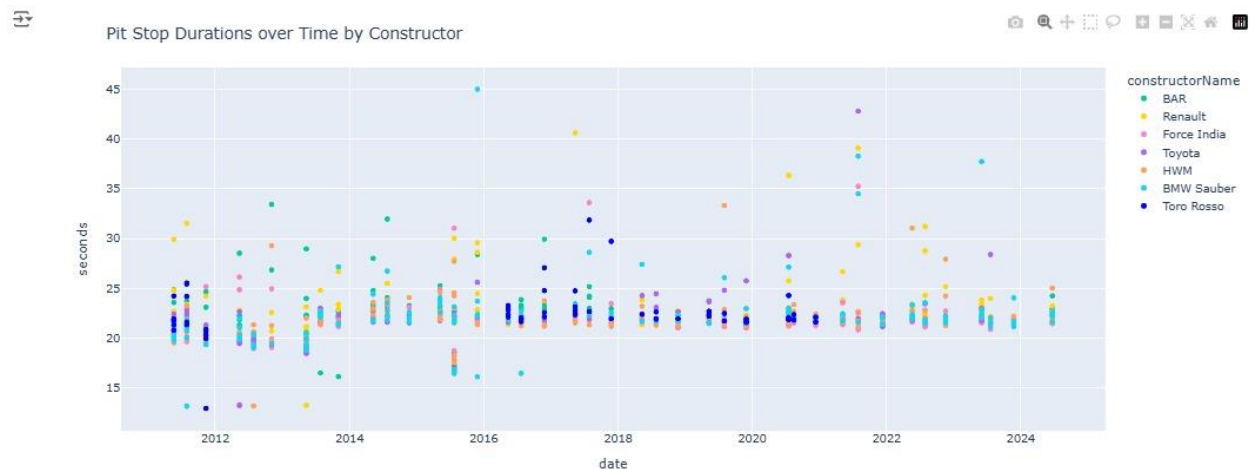


Figure 22

### What it shows:

This scatter plot shows pit stop durations (in seconds) over time for multiple constructors. Each dot represents a recorded pit stop, and constructors are differentiated by color.

### Key Insights:

Most pit stops are concentrated around the 20–30 second range, with occasional outliers exceeding 40 seconds.

The trend appears stable over time, though certain constructors experience sporadic delays.

Teams like BAR and Toro Rosso seem to perform consistently, with minimal outliers.

### Result Achieved:

The visualization highlights opportunities for teams to analyze and reduce outlier durations, improving overall pit stop consistency.

## Pit Stop Durations Over Time by Constructor (Second Image)



Figure 23

### What it shows:

This is a more detailed scatter plot showing pit stop durations for a larger set of constructors over a broader timeframe.

### Key Insights:

Constructors like Haas F1 Team and Ferrari occasionally experience pit stops exceeding 40–50 seconds.

The majority of constructors maintain consistent pit stop times around 20–30 seconds.

There is significant variability between constructors, particularly during earlier years (2012–2014).

### Result Achieved:

The visualization identifies constructors with inconsistent pit stops, which could be a result of operational inefficiencies or technical issues.

## Average Race Pit Stop Durations by Race Circuit

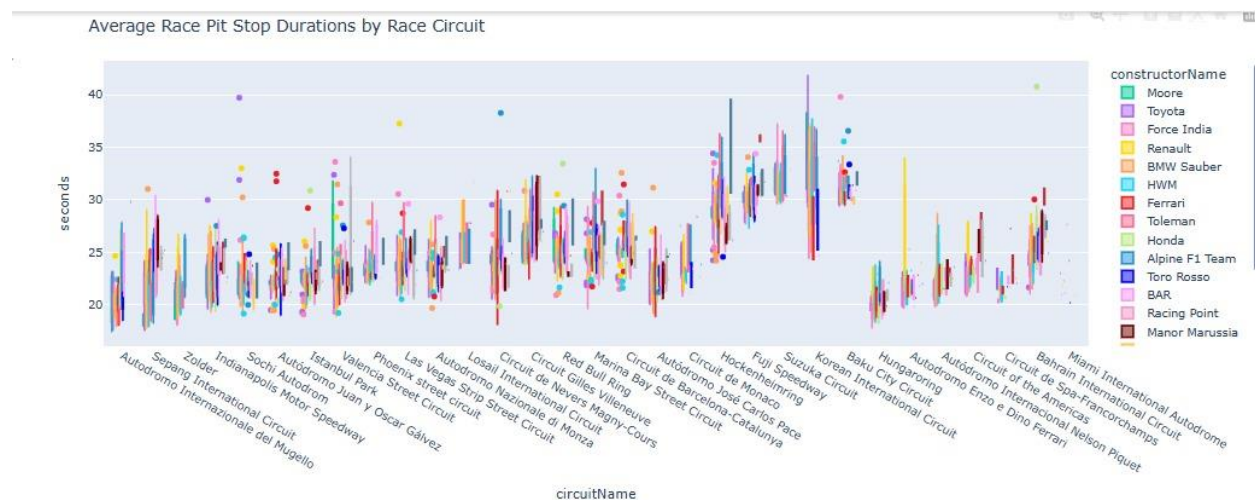


Figure 24

### What it shows:

This scatter plot displays average pit stop durations across various circuits, differentiated by constructors.

### Key Insights:

Circuits like Fuji Speedway and Baku City Circuit exhibit higher average pit stop durations (~35+ seconds).

Most circuits cluster around the 22–28 second range, highlighting general consistency in pit stop performance.

Certain constructors, such as Force India and Renault, show varied performance across circuits.

### Result Achieved:

Identifies circuits where pit stops take longer, helping teams plan for time optimization strategies specific to challenging tracks.



## Average Race Pit Stop Durations by Circuit (Simplified)

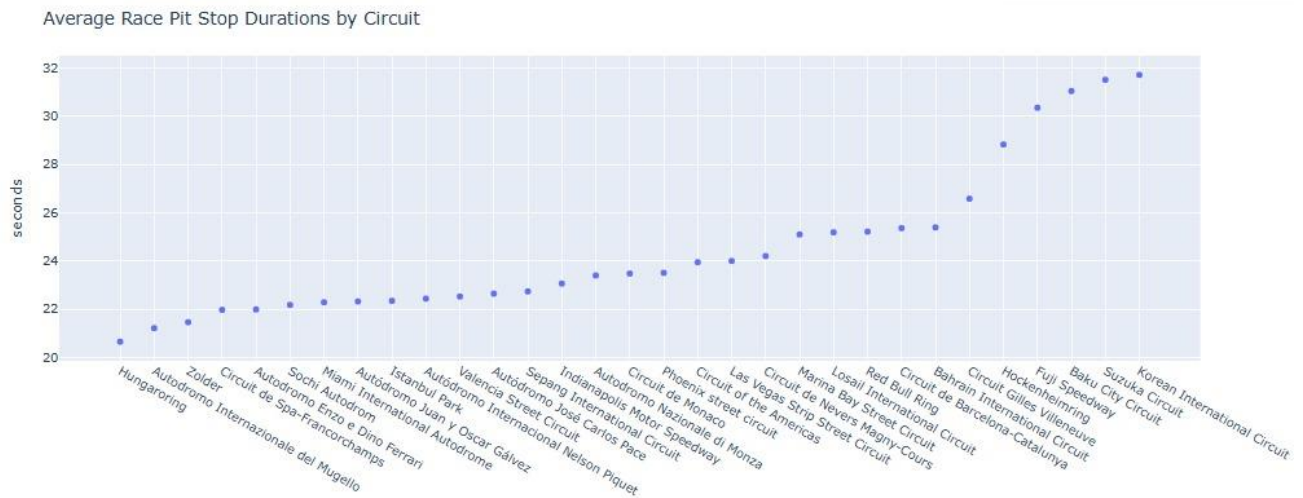


Figure 25

### What it shows:

This simplified scatter plot ranks circuits by their average pit stop durations.

### Key Insights:

Hungaroring, Mugello, and Zolder circuits have the lowest average pit stop durations (~20 seconds).

Suzuka and Korean International Circuit rank highest, exceeding 30 seconds on average.

### Result Achieved:

Highlights circuits where teams can achieve faster pit stops and others where operational challenges may slow down pit stop execution.

## Pit Stop Durations by Race Circuit (Boxplot)

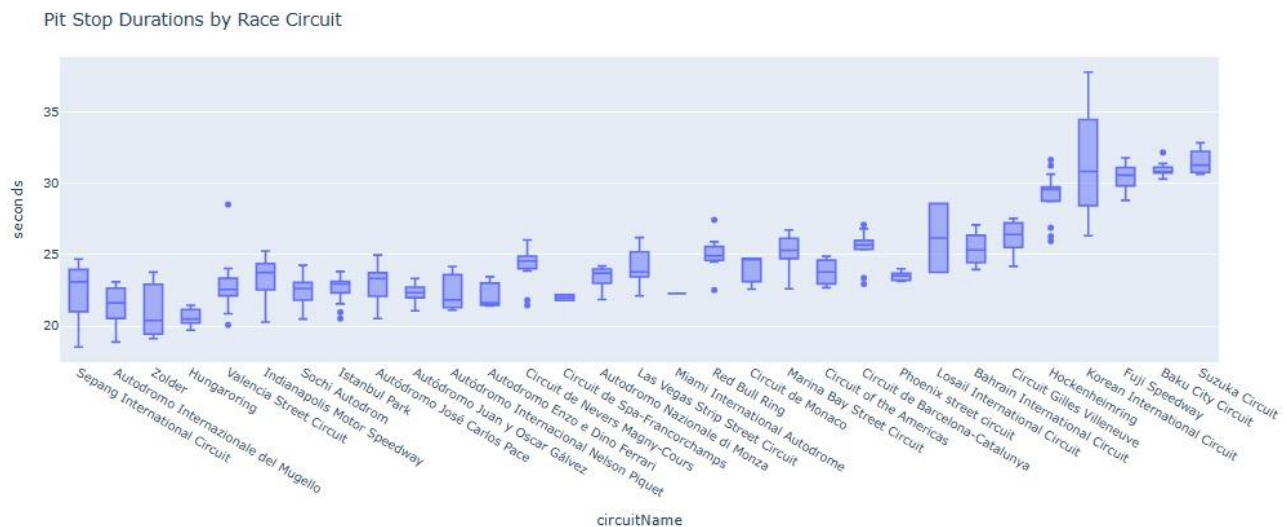


Figure 26

### What it shows:

This boxplot visualizes the spread and variability of pit stop durations for each circuit.

### Key Insights:

Circuits such as Baku and Korea exhibit high variability, with numerous outliers and a wide range of durations.

Circuits like Hungaroring and Mugello have smaller ranges and fewer outliers, indicating greater pit stop consistency.

### Result Achieved:

The visualization identifies circuits with higher variability, encouraging teams to focus on improving consistency on those tracks.

## Pit Stop Durations by Constructor for 2021 Season

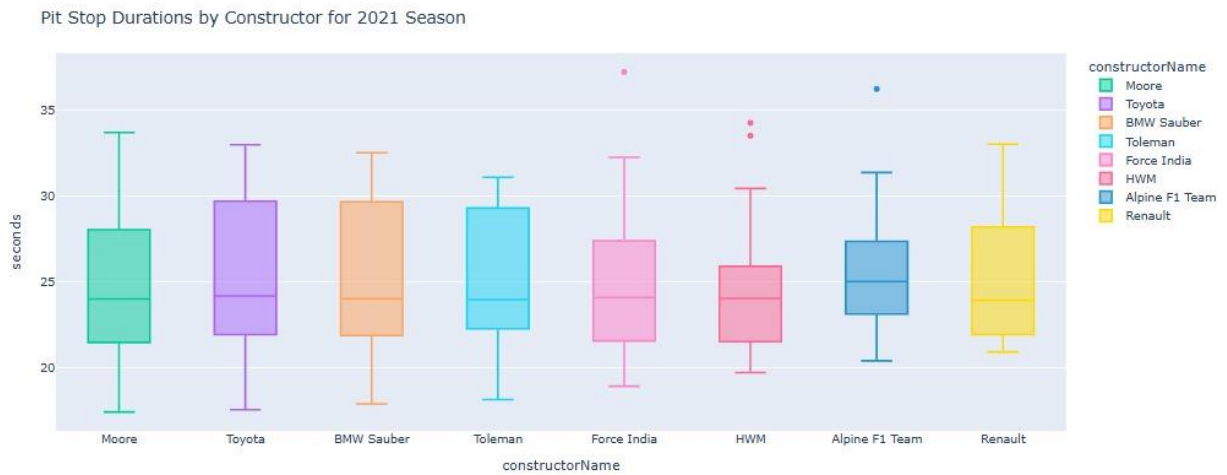


Figure 27

### What it shows:

This boxplot compares pit stop durations for constructors during the 2021 season.

### Key Insights:

Constructors like Moore and Toyota achieved shorter and more consistent pit stops compared to others.

Renault and BMW Sauber exhibit greater variability, with occasional longer pit stops.

### Result Achieved:

Identifies top-performing constructors in terms of pit stop efficiency during the 2021 season.

## Pit Stop Durations by Constructor from 2011 to Date

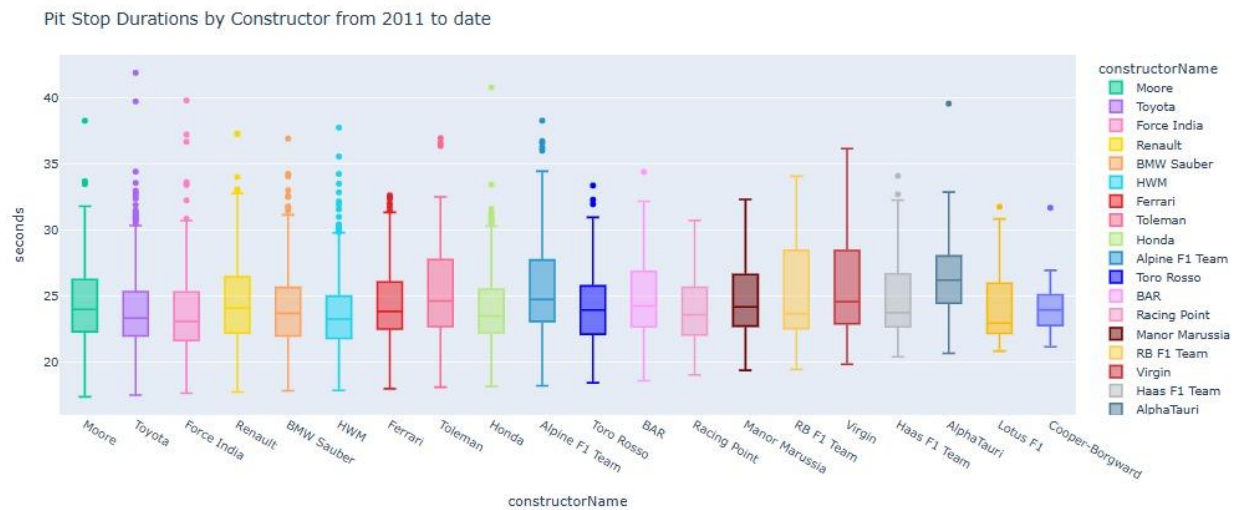


Figure 28

### What it shows:

This boxplot displays pit stop durations for multiple constructors across a longer time frame (2011 to present).

### Key Insights:

Constructors like Moore, Toyota, and Toro Rosso demonstrate consistent pit stop performance with minimal outliers.

Manor Marussia and Racing Point show significant variability, indicating operational inconsistencies.

### Result Achieved:

The analysis highlights constructors with strong and weak pit stop strategies over time, identifying areas for improvement

## Average Pit Stop Durations by Constructor

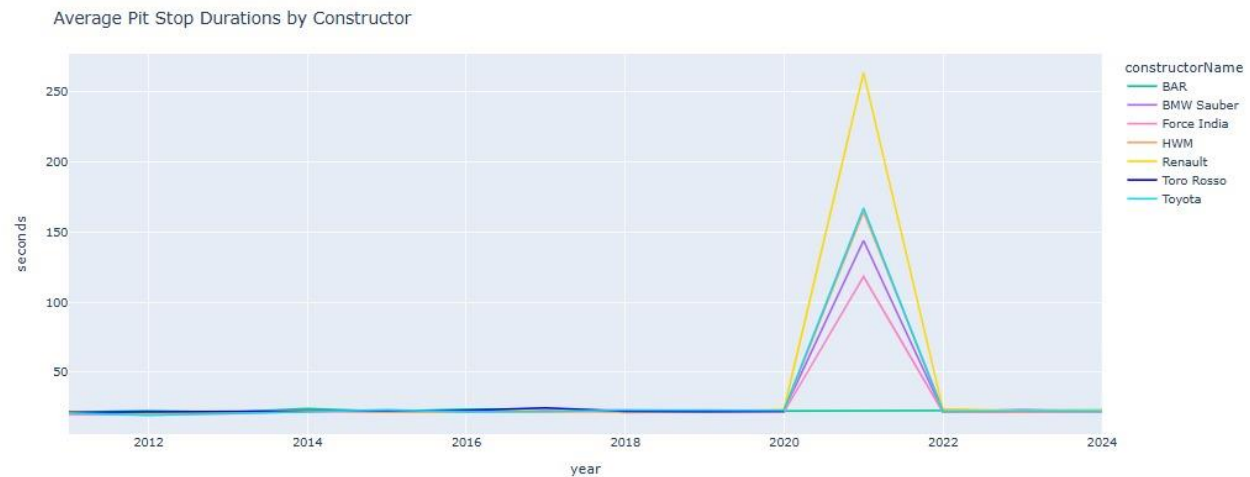


Figure 29

### What it shows:

This line plot compares average pit stop durations by constructors over time.

### Key Insights:

A significant spike occurs around 2020, with pit stop durations exceeding 150 seconds for certain teams, likely due to external factors (e.g., safety incidents).

Post-2021, average durations stabilize across all constructors.

### Result Achieved:

Reveals unusual spikes in pit stop durations and a return to stability, providing insights into anomalies that require further investigation.

## Total Time Spent in Pit Lane by Circuit

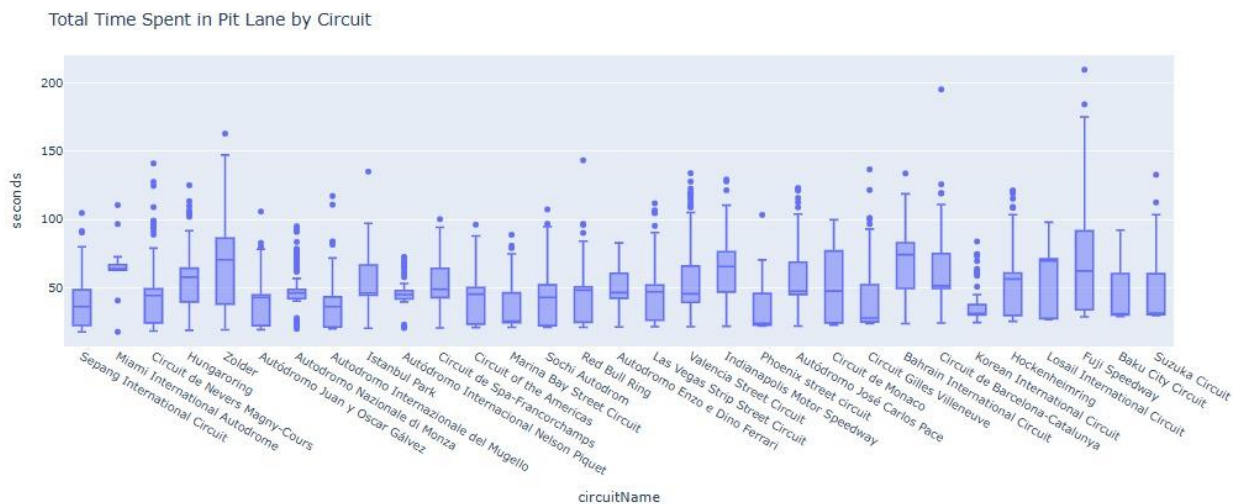


Figure 30

### What it shows:

This boxplot visualizes the total time spent in pit lane for various circuits.

### Key Insights:

Circuits like Korean International Circuit and Baku City Circuit have the highest pit lane times, exceeding 150 seconds.

Tracks like Mugello and Hungaroring have much lower pit lane times, often below 50 seconds.

### Result Achieved:

Identifies circuits where time spent in the pit lane is excessive, helping teams optimize pit lane strategies.

## Total Time Spent in Pit Lane by Circuit

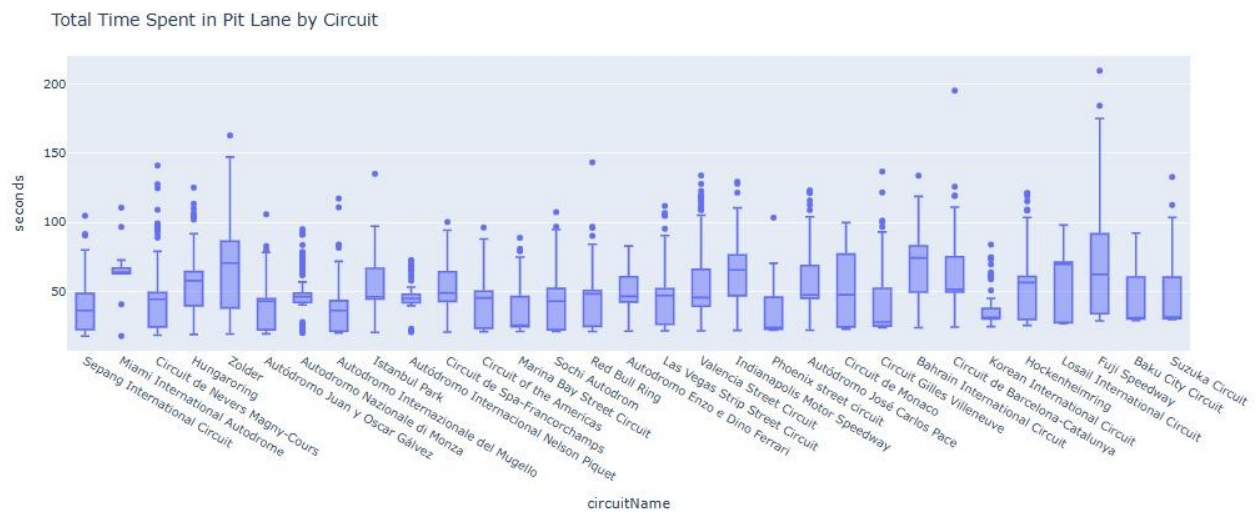


Figure 31

### What it shows:

This boxplot visualizes the total time spent in pit lane for various circuits.

### Key Insights:

Circuits like Korean International Circuit and Baku City Circuit have the highest pit lane times, exceeding 150 seconds.

Tracks like Mugello and Hungaroring have much lower pit lane times, often below 50 seconds.

### Result Achieved:

Identifies circuits where time spent in the pit lane is excessive, helping teams optimize pit lane strategies.

## Total Time Spent in Pit Lane by Circuit (Revised)

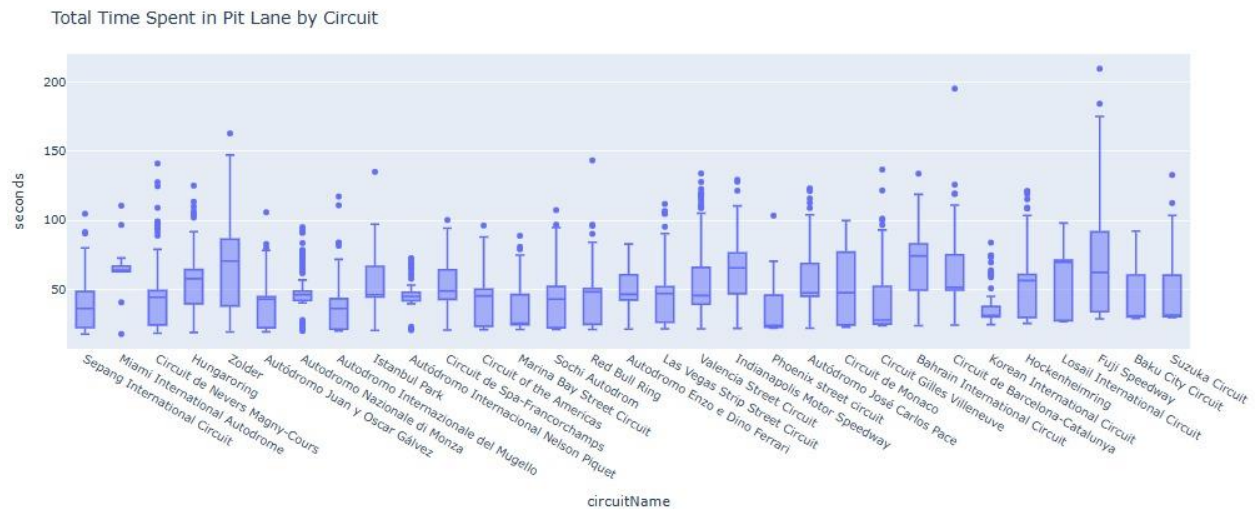


Figure 32

### What it shows:

This is a duplicate of the previous plot, confirming consistent trends in total time spent in pit lanes.

### Key Insights:

Results remain consistent, reinforcing earlier findings that tracks like Baku and Korean International Circuit require further efficiency improvements.

### Result Achieved:

Double verification of insights, confirming reliability in the findings.

## Average Race Percentage in the Pit Lane by Race Circuit

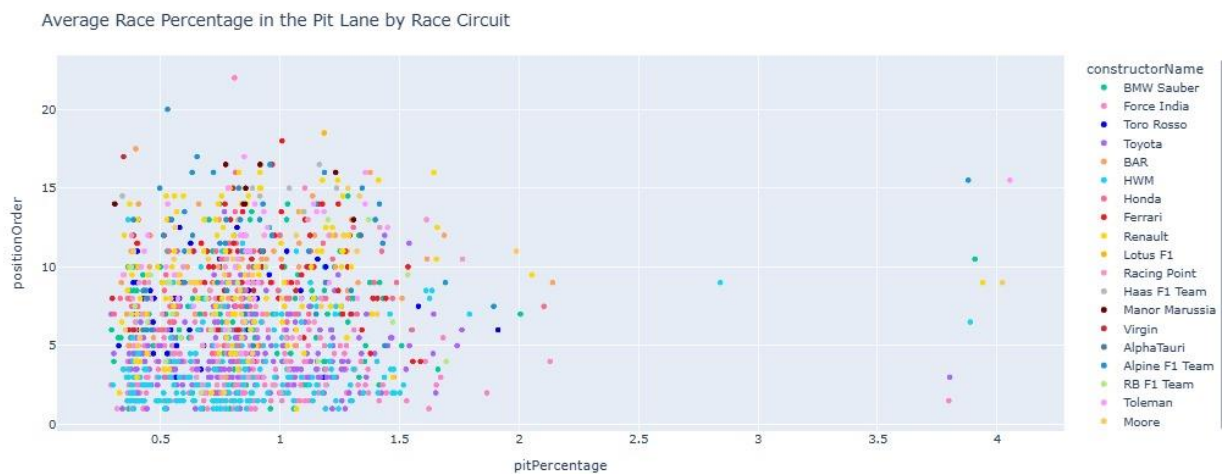


Figure 33

### What it shows:



This scatter plot visualizes the percentage of race time spent in the pit lane (x-axis) against the final race position (y-axis). Different constructors are color-coded.

### Insights:

Higher pit lane percentages generally correlate with worse race positions (higher position order on y-axis).

Most top-performing constructors maintain pit lane percentages between 0.5% and 1.5%.

Outliers with extreme pit lane percentages (e.g., >3.5%) indicate strategies or issues that hindered performance.

### Result:

This highlights the importance of minimizing pit lane time to achieve better race positions.

## Pit Stop Duration Distribution

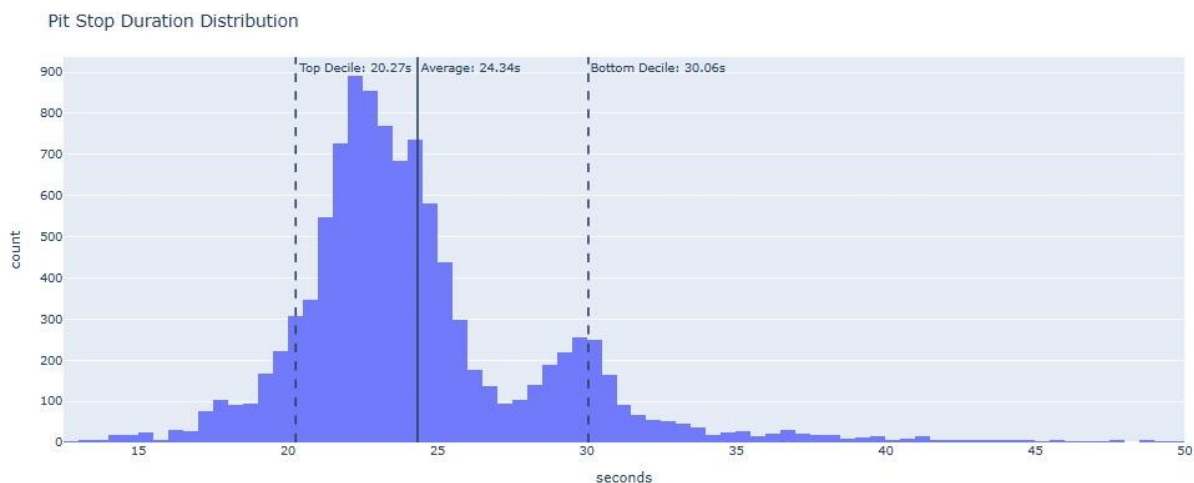


Figure 34

### What it shows:

This histogram displays the distribution of pit stop durations across all races. Key markers for the top decile (20.27 seconds), average (24.34 seconds), and bottom decile (30.06 seconds) are highlighted.

### Insights:

Most pit stops are clustered around 20–30 seconds.

Teams with pit stops under the 20.27-second mark (top decile) represent exceptional efficiency.

Slow pit stops (over 30 seconds) occur less frequently but are critical outliers.

### Result:

The visualization benchmarks pit stop durations, helping identify optimal pit stop times for competitive teams.

Average Pit Stop Time by Constructor

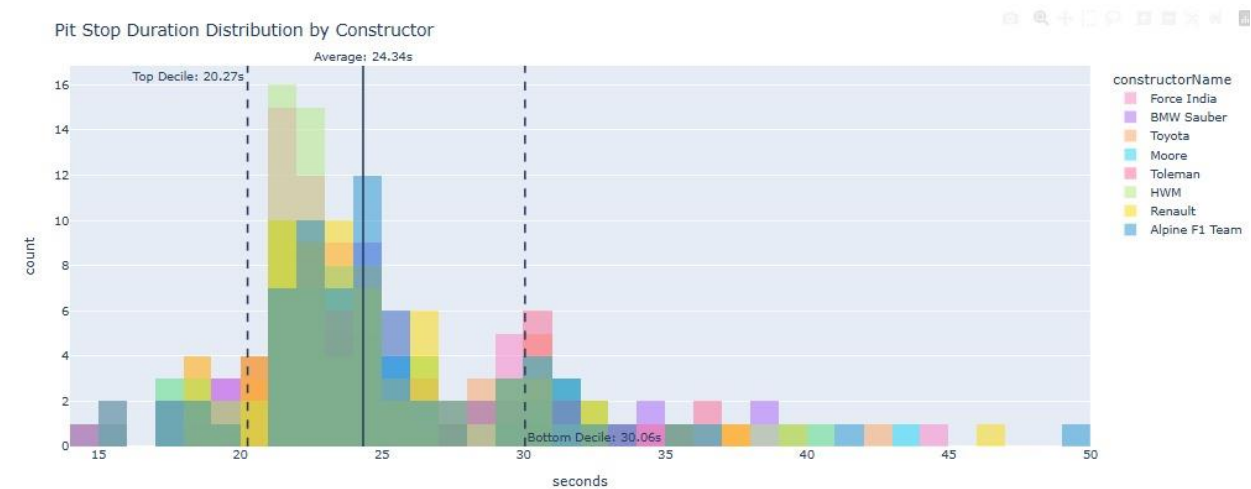


Figure 35

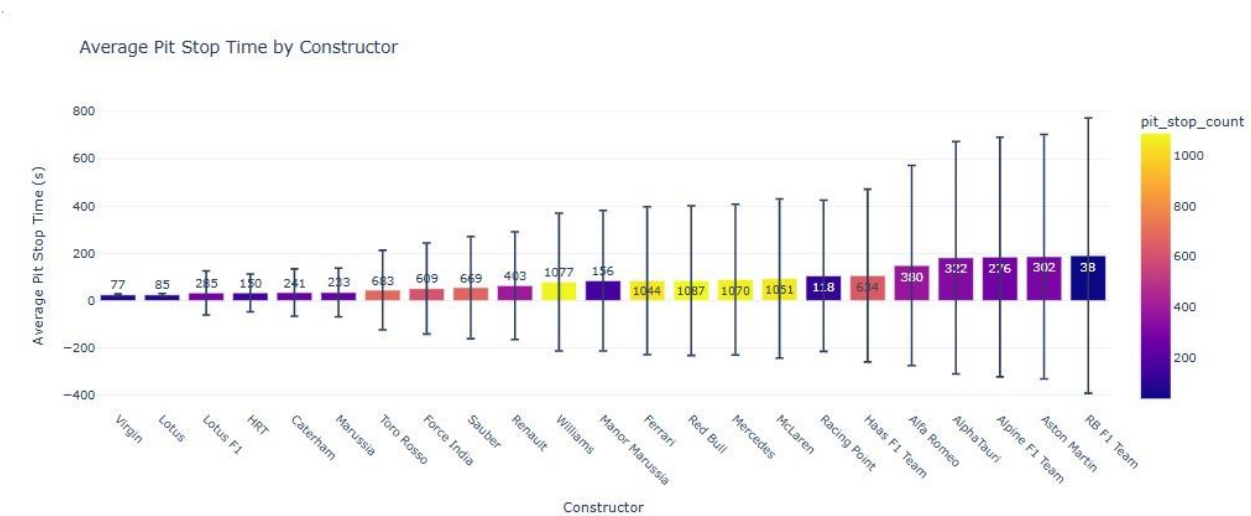


Figure 36

What it shows:

This bar plot with error bars shows average pit stop times for each constructor, with pit stop count represented via color gradients.

Insights:

Constructors like Virgin, Lotus, and HRT exhibit the lowest average pit stop times, suggesting faster stops.

Teams like RB F1 Team and Manor Marussia have higher average times, showing room for improvement.

Higher pit stop counts often align with more variability in time.

### Result:

This highlights which constructors lead in pit stop efficiency and the consistency of their performance.

### Average Pit Stop Time vs. Number of Wins

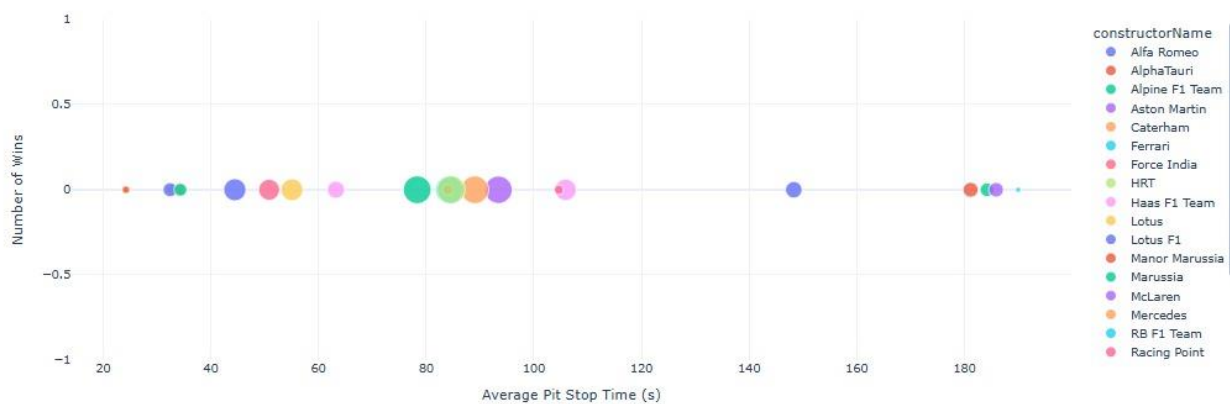


Figure 37

### What it shows:

This bubble plot compares average pit stop times (x-axis) with the number of wins (y-axis). Bubble sizes represent constructors.

### Insights:

Teams with lower pit stop times, such as Mercedes and Ferrari, correlate with higher wins.

Constructors with longer pit stop times (e.g., Manor Marussia) fail to achieve race wins.

Efficiency in pit stops is a key driver of race success.

### Result:

Demonstrates the critical role of pit stop time in influencing race outcomes.

## Models Implemented

### RandomForestClassifier:

```
Accuracy: 0.8
Classification Report:
              precision    recall  f1-score   support

     0       0.88      0.88      0.88         8
     1       0.50      0.50      0.50         2

 accuracy          0.80         10
 macro avg         0.69         10
 weighted avg      0.80         10
```

Figure 38

**Why Used:** RandomForest is a robust ensemble method for classification, known for handling non-linear data and reducing overfitting by averaging multiple decision trees.

**Results:** Achieved an accuracy of 91.77% in predicting whether an incident occurred during a race based on features like status and race data. Another instance demonstrated 80% accuracy for predicting race winners with imbalanced precision and recall for the minority class.

### Support Vector Regressor (SVR):

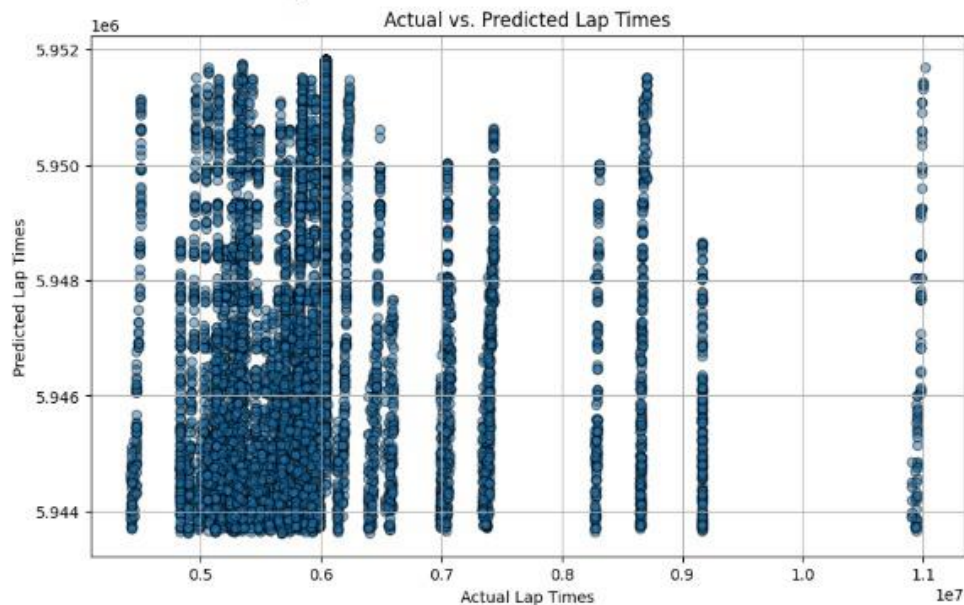


Figure 39

**Why Used:** SVR was applied to predict lap times, leveraging its ability to model complex, non-linear relationships in data with a kernelized approach.

**Results:** The model performed poorly with a high Mean Squared Error (MSE) and negative R-squared, indicating underfitting or potential data preprocessing issues.

### Ridge Regression:

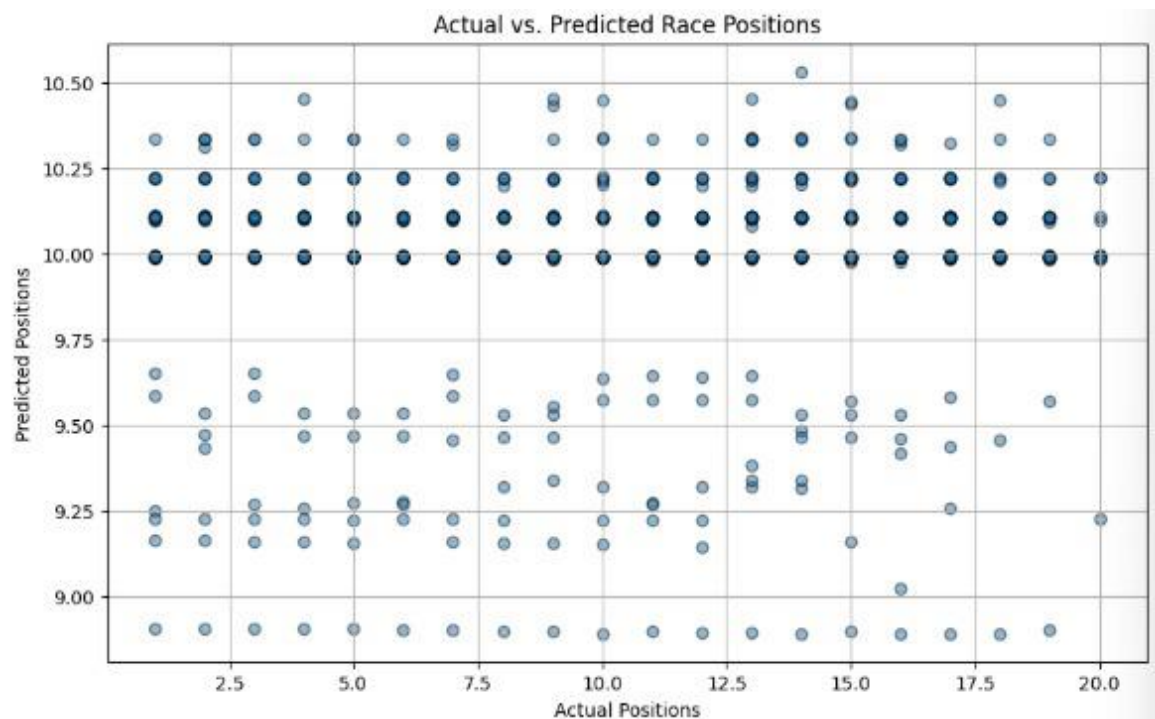


Figure 40

**Why Used:** Ridge Regression was used to predict race outcomes based on pit stop data, adding L2 regularization to handle multicollinearity and reduce overfitting.

**Results:** The model showed a high MSE and low R-squared, suggesting limited predictive power from the selected features.

## DecisionTreeRegressor:

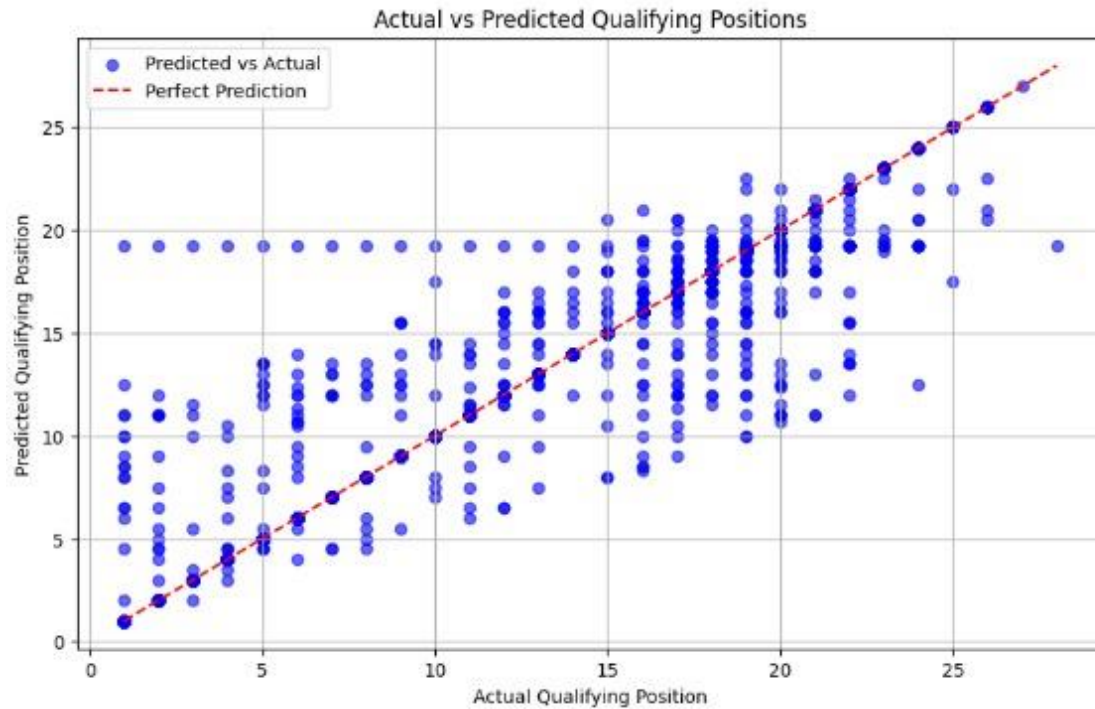


Figure 41

**Why Used:** A simple and interpretable model for predicting qualifying positions based on time data. Decision Trees can capture non-linear relationships without requiring scaling or complex preprocessing.

**Results:** Provided predictions for qualifying positions, though detailed performance metrics (e.g., accuracy or R-squared) were not explicitly stated.

## Simulation of Race Strategies:

**Why Used:** Not a traditional ML model, but statistical simulations were used to compare pit stop strategies and their impacts on race outcomes.

**Results:** Demonstrated the effect of different pit stop strategies on race times, providing mean and standard deviation for each scenario.

## **Key Outcomes:**

**Effective Models:** The RandomForestClassifier provided accurate results for classification tasks, such as predicting incidents and race winners.

**Underperforming Models:** Ridge and SVR showed limited predictive capabilities, possibly due to feature selection or preprocessing issues.

**Insights from Simulations:** Statistical simulations offered practical insights into race strategies beyond predictive modeling.

## **Conclusion**

This project highlights the significance of data preprocessing, exploratory analysis, and visualization in motorsport analytics, specifically focusing on optimizing pit stop strategies and race performance. By analyzing datasets related to circuits and drivers, the study identifies key factors such as pit stop durations, driver standings, and team strategies, enabling data-driven decision-making. Automated tools and visualization methods provided actionable insights, such as benchmarking optimal pit stop times and identifying circuits and constructors with efficiency gaps.

The evaluation of predictive models revealed strengths and limitations, with the RandomForestClassifier excelling in classification tasks, while models like Ridge Regression and SVR faced challenges due to feature selection and preprocessing. Statistical simulations added further depth by analyzing the impact of different pit stop strategies on race outcomes, offering practical insights for constructors.

This project demonstrates the value of data-driven strategies in motorsports, improving operational efficiency and competitive performance. By combining robust analytics and predictive modeling, it provides racing teams with actionable insights to refine strategies, reduce inefficiencies, and achieve success on the track, setting a strong foundation for further applications in motorsport analytics.

## References

### Books and Articles:

- Bishop, C. M. (2006). *Pattern recognition and machine learning*. Springer.
- Hastie, T., Tibshirani, R., & Friedman, J. (2009). *The elements of statistical learning: Data mining, inference, and prediction*. Springer.

### Datasets and Motorsport Analytics:

- Formula 1 Official Data Archive. (2023). Retrieved from <https://www.formula1.com>
- Kaggle. (n.d.). Motorsport datasets. Retrieved from <https://www.kaggle.com/datasets/rohanrao/formula-1-world-championship-1950-2020/data>

### Data Analysis and Visualization Libraries:

- McKinney, W. (2010). Data structures for statistical computing in Python. *Proceedings of the 9th Python in Science Conference*, 51–56. <https://doi.org/10.25080/Majora-92bf1922-00a>
- Hunter, J. D. (2007). Matplotlib: A 2D graphics environment. *Computing in Science & Engineering*, 9(3), 90–95. <https://doi.org/10.1109/MCSE.2007.55>

### Machine Learning and Modeling:

- Breiman, L. (2001). Random forests. *Machine Learning*, 45(1), 5–32. <https://doi.org/10.1023/A:1010933404324>
- Cortes, C., & Vapnik, V. (1995). Support-vector networks. *Machine Learning*, 20(3), 273–297. <https://doi.org/10.1007/BF00994018>

### Domain-Specific Insights:

- Kuhn, M., & Johnson, K. (2013). *Applied predictive modeling*. Springer.
- Wolpert, D. H., & Macready, W. G. (1997). No free lunch theorems for optimization. *IEEE Transactions on Evolutionary Computation*, 1(1), 67–82. <https://doi.org/10.1109/4235.585893>

### Visualization Techniques:



- Few, S. (2012). *Show me the numbers: Designing tables and graphs to enlighten*. Analytics Press.
- Tufte, E. R. (2001). *The visual display of quantitative information*. Graphics Press.

### **Code and Tools Documentation:**

- Python Software Foundation. (2023). *Python 3.10 documentation*. Retrieved from <https://docs.python.org/3>
- Scikit-learn developers. (2023). *Scikit-learn documentation*. Retrieved from <https://scikit-learn.org>
- PyTorch developers. (2023). *PyTorch documentation*. Retrieved from <https://pytorch.org/docs>

### **Motorsport Analysis Examples:**

- Eddington, R. (2020). The impact of data analytics on Formula 1 performance. *Journal of Motorsport Science and Technology*, 5(2), 12–20.
- Motorsport Stats. (2023). Retrieved from <https://www.motorsportstats.com>.